Table 1. Effect of 4-Aminopyridine, Tertiapin and NIP-142 on Mouse Atrial Action Potential Duration

		4-Aminopyridine (1 mM)	4-Aminopyridine (10 mM)	Tertiapin (1 μM)	NIP-142 (1 μM)	NIP-142 (10 μM)	NIP-142 (100 μM)
APD_{20} (ms)	Before	3.3±0.4	4.4±0.3	2.4±0.2	2.7±0.4	2.6±0.1	2.7±0.2
	After	8.5±0.4*	18.6±1.3*	2.5±0.3	2.6±0.3	3.5±0.2*	12.7±2.1*
APD_{90} (ms)	Before	32.8±2.2	36.2±2.1	39.1±2.9	33.2±3.7	33.0±2.9	35.0±2.3
	After	32.8±1.9	60.0±3.1*	59.8±3.8*	34.7±4.0	44.9±1.5*	90.5±6.3*

Action potential duration at 20% repolarization (APD_{20}) and 90% repolarization (APD_{90}) were measured before and 30 min after the addition of 1 mM or 10 mM 4-aminopyridine, 1 μM tertiapin, and 1 to 100 μM NIP-142. Values indicate the mean±S.E.M. from 4 to 5 experiments. Asterisks on values after addition indicate significant difference ($p<0.05$) from corresponding values before addition as determined by the paired t-test.

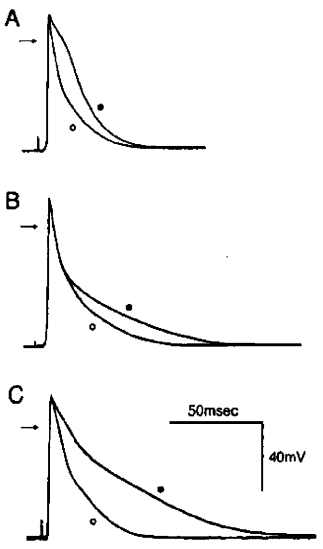

Fig. 2. Effect of 4-Aminopyridine, Tertiapin and NIP-142 on Mouse Atrial Action Potential

Typical action potential records obtained in the absence (open circles) and presence (closed circles) of 1 mM 4-aminopyridine (A), 1 μM tertiapin (B) and 100 μM NIP-142 (C). Arrows indicate zero mV level.

142 (100 μM) prolonged the effective refractory period of isolated mouse atria from 43.0±2.6 ms to 71.0±5.1 ms ($n=5$); the increase was statistically significant. 4-Aminopyridine, 1 mM and 10 mM, increased the contractile force from 122.3±25.9 mg to 219.3±42.6 mg (184%) and 359.5±50.3 mg (319%), respectively ($n=5$); the increases were statistically significant.

DISCUSSION

NIP-142 concentration-dependently blocked the Kv1.5, Kv4.2 and Kv4.3 potassium channel currents (Fig. 1). These currents are considered to be the major repolarizing currents in the rodent myocardium and also to contribute to repolarization in the myocardium of many species including human. NIP-142 was shown to block the repolarizing outward currents in human atrial cardiomyocytes, but the molecular target of the blocking effect had not been clarified.[7] The present results show that NIP-142 blocks the Kv1.5, Kv4.2 and Kv4.3 channel currents (Fig. 1), the inhibitory effect of 100 μM NIP-142 on Kv1.5 was larger than that on Kv4.2 and Kv4.3. We have previously reported the inhibitory action of NIP-142 on human Kv1.5.[10] The potency of NIP-142 on human Kv1.5 was slightly higher than in the present study with mouse Kv1.5, which may reflect species difference in the structure of the Kv1.5 channel. Alternatively, the difference in potency may be due to the difference in expression systems; human Kv1.5 in our previous study was expressed in HEK293 cells, which is generally known to result in higher sensitivity of expressed ion channel to inhibitory agents compared with the *Xenopus* oocyte system.

The mRNAs for Kv1.5, Kv4.2 and Kv4.3, which underlie the transient outward current, is detected both in human[11] and mouse atria.[12] The mouse atrium has a larger transient outward current-density[7,12] and shorter action potential duration[12,13] than the human atrium. Prolongation by 1 mM and 10 mM 4-aminopyridine of the early repolarization phase of the mouse atrial action potential (Table 1; Fig. 1A) indicates that the transient outward current through Kv1.5, Kv4.2 and Kv4.3 channels is the major determinant of early repolarization.[14] Thus, the mouse atrial myocardium provides an experimental model to study the effect of agents modifying these channels.[15] NIP-142 was shown to prolong the early phase repolarization indicating that it indeed blocks the transient outward current in the atrial cardiomyocyte. The late repolarization, on the other hand, appears to be influenced by currents dominating in the voltage range more negative than −40 mV including the acetylcholine-activated potassium current. In guinea-pig myocardium, we have shown that the acetylcholine-activated potassium current is present in the atrial myocardium in the absence of muscarinic receptor stimulation, and that NIP-142 prolongs action potential duration and effective refractory period through blockade of this current.[6,8] Such effect was not observed in the ventricle which may explain the atria-selective nature of NIP-142. Also in the case of the mouse atrium, NIP-142, as well as tertiapin, a peptide inhibitor of the acetylcholine-activated potassium channel, prolonged the late repolarization phase (Figs. 2B, C). NIP-142 was shown to inhibit the acetylcholine-activated potassium channel current and prolong the action potential duration in guinea-pig atrial myocardium.[8] Thus, although further investigation is necessary for definitive conclusions, the most likely explanation for the effects of NIP-142 in mouse atria at present is that NIP-142 prolongs the atrial action potential duration through blockade of the transient outward current as well as the acetylcholine-activated potassium current, and produces prolongation of the effective refractory period.

Blockade of Kv1.5, Kv4.2 and Kv4.3 appears to be advantageous for the treatment of atrial fibrillation. It is well known that atrial arrhythmias are closely associated with pathological conditions including atrial dilatation.[16] Atrial

stretch exerts short-term and long-term effects on ion channel expression leading to shortening of the action potential duration and refractory period.[17] It was reported that 4-aminopyridine could counteract the shortening of action potential duration and effective refractory period induced by application of stretch to atrial myocytes.[18] Many studies support the hypothesis that in patients of atrial fibrillation, loss of atrial contractile function causing stasis of blood near the atrial wall is one of the important mechanisms of atrial thrombus formation.[19,20] Blockade of the transient outward current may be an effective strategy to inhibit atrial thrombus formation if it could increase atrial contractility. It was indeed reported that AVE0118, a blocker of the transient outward and ultrarapid delayed rectifier current, fully restored atrial contractility after cardioversion of atrial fibrillation in the goat without proarrhythmic effects on the ventricle.[21] In the present study, 1 mM 4-aminopyridine, which blocks the Kv1.5 channel current, and 10 mM 4-aminopyridine, which also blocks the Kv4.2 and Kv4.3 channel currents, gradually increased the atrial contractile force. Although details await further investigation, NIP-142, which prolonged action potential duration and increased atrial contractile force through inhibition of these currents, might also have these beneficial effects.

In conclusion, NIP-142 was shown to inhibit the Kv1.5, Kv4.2 and Kv4.3 channel current. This effect, and the blockade of acetylcholine-activated potassium current, may contribute to the prolongation of effective refractory period by NIP-142.

Acknowledgments This study was supported in part by the Science Research Promotion Fund from the Promotion and Mutual Aid Corporation for Private Schools of Japan (for YT and HT). This study was partly performed as a part of the project "Research on the molecular mechanisms of appearance of age-related diseases by failure of cell function control system, and their prevention and treatment" by the "Research Center for Aging and Age-Related Diseases" established in the Toho University Faculty of Pharmaceutical Sciences.

REFERENCES

1) Sugimoto T., Hayakawa K. and Kasanuki H., "Atrial Fibrillation, Flutter, and Tachycardia," ed. by Hayakawa K., Kasanuki H., Igaku-Shoin, Tokyo, 1999, pp. 14—18.
2) Aliot E., Denjoy I., *Am. J. Cardiol.*, **77**, 66A—71A (1996).
3) Iwasaki H., Takahara A., Nakamura Y., Satoh Y., Nagai T., Shinkai N., Sugiyama A., *J. Pharmacol. Sci.*, **110**, 410—414 (2009).
4) Lenz T., Hilleman D., *Drugs Today* (Barc), **36**, 759—771 (2000).
5) Nagasawa H., Fujiki A., Fujikura N., Matsuda T., Yamashita T., Inoue H., *Circ. J.*, **66**, 185—191 (2002).
6) Matsuda T., Takeda K., Ito M., Yamagishi R., Tamura M., Nakamura H., Tsuruoka N., Saito T., Masumiya H., Suzuki T., Iida-Tanaka N., Itokawa M., Yamashita T., Tsuruzoe N., Tanaka H., Shigenobu K., *J. Pharmacol. Sci.*, **98**, 33—40 (2005).
7) Seki A., Hagiwara N., Kasanuki H., *J. Cardiovasc. Pharmacol.*, **39**, 29—38 (2002).
8) Matsuda T., Ito M., Ishimaru S., Tsuruoka N., Saito T., Iida-Tanaka N., Hashimoto N., Yamashita T., Tsuruzoe N., Tanaka H., Shigenobu K., *J. Pharmacol. Sci.*, **101**, 303—310 (2006).
9) Nishimaru K., Makuta R., Tanaka Y., Tanaka H., Shigenobu K., *Pharmacology*, **62**, 87—91 (2001).
10) Matsuda T., Masumiya H., Tanaka N., Yamashita T., Tsuruzoe N., Tanaka Y., Tanaka H., Shigenobu K., *Life Sci.*, **68**, 2017—2024 (2001).
11) Gaborit N., Bouter S.L., Szuts V., Varro A., Escande D., Nattel S., Demolombe S., *J. Physiol.*, **582**, 675—693 (2007).
12) Trépanier-Boulay V., Lupien M., St-Michel C., Fiset C., *Cardiovasc. Res.*, **64**, 84—93 (2004).
13) Wang Y., Xu H., Kumar R., Tipparaju S. M., Wagner M. B., Joyner R. W., *J. Mol. Cell. Cardiol.*, **35**, 1083—1092 (2003).
14) Oudit G. Y., Kassiri Z., Sah R., Ramirez R. J., Zobel C., Backx P. H., *J. Mol. Cell. Cardiol.*, **33**, 851—872 (2001).
15) Tanaka H., Namekata I., Nouchi H., Shigenobu K., Kawanishi T., Takahara A., *J. Pharmacol. Sci.*, **109**, 327—333 (2009).
16) Fukuda T., Yamashita T., Sagara K., Kato T., Sawada H., Aizawa T., *Circ. J.*, **71**, 308—312 (2007).
17) Kalifa J., Jalife J., Zaitsev A. V., Bagwe S., Warren M., Moreno J., Berenfeld O., Nattel S., *Circulation*, **108**, 668—671 (2003).
18) Qi J., Xiao J., Zhang Y., Li J., Liu Y., Li P., Liang L., Jiang B., Wen W., Zhao C., Liang D., Liu Y., Chen Y. H., *Exp. Biol. Med.*, **234**, 779—784 (2009).
19) Fatkin D., Kelly R. P., Feneley M. P., *J. Am. Coll. Cardiol.*, **23**, 961—969 (1994).
20) Mugge A., Kuhn H., Nikutta P., Grote J., Lopez J. A., Daniel W. G., *J. Am. Coll. Cardiol.*, **23**, 599—607 (1994).
21) deHaan S., Greiser M., Harks E., Blaauw Y., Hunnik A., Verheule S., Allessie M., Schotten U., *Circulation*, **114**, 1234—1242 (2006).

H_2 Receptor-Mediated Positive Inotropic Effect of Histamine in Neonatal Guinea-Pig Left Atria

Naoki AGATA,[a] Yoshimitsu KATO,[a] Iyuki NAMEKATA,[a] Akira TAKAHARA,[a] Hikaru TANAKA,*[,a] Daisuke CHINO,[b] Katsuo KOIKE,[c] and Yoshio TANAKA[c]

[a] *Department of Pharmacology, Faculty of Pharmaceutical Sciences, Toho University;* [c] *Department of Chemical Pharmacology, Faculty of Pharmaceutical Sciences, Toho University; Funabashi, Chiba 274–8510, Japan; and* [b] *Department of Pharmacology, School of Medicinal Pharmacy, Nihon Pharmaceutical University; Kitaadachi-gun, Saitama 362–0806, Japan.* Received August 20, 2010; accepted September 4, 2010; published online September 8, 2010

The receptor type mediating the positive inotropic effect of histamine was examined in left atria from neonatal guinea pigs. The positive inotropic effect of histamine, as well as its action potential prolonging effect, was antagonized by ranitidine, but not by chlorpheniramine or thiperamide. The positive inotropic effect was enhanced by isobutylmethylxantine. Receptor binding studies revealed the presence of both H_1 and H_2 receptor types. These results suggest that the positive inotropic effect of histamine in the neonatal guinea-pig atrium is mediated by H_2 receptors.

Key words histamine; inotropy; guinea-pig; left atrium; neonate

Histamine is present in high concentrations in the myocardium of most animal species including human, and its release and subsequent actions on the myocardium is considered to be of importance under certain pathological conditions such as arrhythmia and septic shock.[1—4] Histamine is known to produce increase in sinus rate and ventricular automaticity, a decrease in atrio-ventricular conduction velocity, and an increase in myocardial contractility through its direct action on cardiomyocytes. In some cases, histamine influences myocardial contractility through release of transmitters from autonomic nerve terminals.[5,6] The direct positive chronotropic and inotropic effects of histamine are principally mediated by activation of H_2 receptors and an increase in intracellular cAMP production, mechanisms analogous to that for β-adrenergic stimulation. However, there seems to be some variation in the type of receptors mediating the positive inotropic effect among animal species, region of the heart, as are often observed with other biologically active substances.[7,8] In case of the adult guinea-pig left atria, histamine shows a positive inotropic effect; this effect was shown to be mediated by H_1 receptors and to be accompanied by prolongation of the action potential.[9—12] The sensitivity to histamine of the left atria was reported to be low in the neonate and to be increased during postnatal development,[13] but whether there are any changes in the mechanisms involved has not yet been clarified. In the present study, we intended to clarify the receptor type involved in the positive inotropic effect of histamine on neonatal atria with contractile force experiments, action potential measurements, and receptor binding assay.

MATERIALS AND METHODS

Experiments with Isolated Guinea-Pig Atria All experiments were approved by the Ethics Committee of Toho University, and were performed in accordance with the "Guiding Principles for the Care and Use of Laboratory Animals" approved by the Japanese Pharmacological Society. The left atria were isolated from neonatal (0 to 1 d old) guinea pigs and measurement of the action potential with standard glass microelectrode techniques and measurement of contractile force were performed as described.[14,15] Briefly, the left atria were placed horizontally in 20 ml organ bath and driven at 1 Hz by field stimulation. Contractile force was measured with an isometric transducer (TB-611T, Nihon Kohden, Tokyo, Japan) connected to a minipolygraph (RM-6100, Nihon Kohden, Tokyo, Japan). Action potentials were recorded with glass microelectrodes connected to a microelectrode amplifier (MEZ-7101, Nihon Kohden, Tokyo, Japan), fed into an AD converter (Analog Pro, Canopus, Kobe, Japan) and digitally analyzed (Analy X, Sawada & Hirano, Tsukuba, Japan).

Preparation of Microsomal Fractions The atria removed from neonatal (0 to 1 d old) guinea-pigs were minced with scissors and homogenized with a Potter–Elveheim homogenizer in 20 volume of 0.25 M sucrose containing 10 mM tris(hydroxymethyl)aminomethane–HCl (Tris–HCl; pH 7.4 at 4 °C). The homogenate was centrifuged at 2500 *g* for 10 min and the supernatant was again centrifuged at 15000 *g* for 20 min. Centrifugation of this supernatant at 100000 *g* for 60 min resulted in a pellet that was suspended in 10 mM Tris–HCl at a concentration of 0.5 to 0.8 mg protein/ml and was used as the microsomal fraction.

Receptor Binding Assay The microsomal fraction was incubated with various concentrations of [^{3}H]mepyramine or [^{3}H]tiotidine in a total volume of 150 μl of incubation buffer (50 mM Tris–HCl, pH 7.4 at 37 °C) for 60 min. The incubation mixture was filtered with Whatman GF/C glass-fiber filters. After the passage, the filters were dried and the radioactivity was measured in a toluene-based scintillator with a liquid scintillation spectrometer (LSC-900, Aloka, Tokyo, Japan). Non-specific binding was determined as radioactivity bound to the microsomal fraction that was not displaced by non-radioactive ligands (30 μM mepyramine or 10 μM cimetidine). Specific binding was obtained as the difference between total binding and non-specific binding. The maximum binding capacity (B_{max}) and the equilibrium dissociation constant (K_d) were calculated from Scatchard analysis of the saturation data.

Drug and Chemicals The drugs used were histamine di-

* To whom correspondence should be addressed. e-mail: htanaka@phar.toho-u.ac.jp

hydrochloride (Wako, Osaka, Japan), chlorpheniramine maleate (Wako, Osaka, Japan), ranitidine hydrochloride (Sigma-Aldrich, St. Louis, MO, U.S.A.), cimetidine (Sigma-Aldrich, St. Louis, MO, U.S.A.), thioperamide maleate (Sigma-Aldrich, St. Louis, MO, U.S.A.), 3-isobutyl-1-methylxanthine (IBMX; Sigma-Aldrich, St. Louis, MO, U.S.A.), ^{3}H-mepyramine (PerkinElmer, Waltham, MA, U.S.A.), and ^{3}H-tiotidine (PerkinElmer, Waltham, MA, U.S.A.). All other chemicals were commercial products of the highest available grade of quality.

Statistical Analysis All experimental data are expressed as mean±standard errors of the mean (S.E.M.). The statistical significance of differences between means was evaluated by the Dunnett's test for multiple comparisons. A value of $p<0.05$ was considered statistically significant.

RESULTS

In isolated neonatal guinea-pig left atria, histamine produced a concentration-dependent positive inotropic effect (Fig. 1A); the pD_2 value was 5.29±0.12 and the contractile force was increased to 253±19.1% of the initial value by 10 μM histamine ($n=5$). The H_2 receptor antagonist ranitidine produced a rightward shift of the concentration–response relationship of histamine. The pD_2 value in the presence of 10 μM ranitidine was 3.81±0.19 ($n=5$) and the calculated pA_2 value was 6.46. In contrast, neither the H_1 antagonist chlorpheniramine nor the H_3 receptor antagonist thioperamide affected the concentration–response relationship; pD_2 values in the presence of 0.3 μM chlorpheniramine and 1 μM thiperamide were 5.04±0.05 and 5.36±0.12, respectively. The phosphodiesterase inhibitor isobutylmethylxantine (IBMX) enhanced the inotropic response to histamine (Fig. 1B).

Histamine prolonged the action potential duration (Fig. 2Aa). The action potential duration at 90% repolarization (APD_{90}) in the absence and presence of 3 μM histamine was 81.6±3.7 ms and 101.0±3.3 ms, respectively ($n=5$). This prolongation of APD_{90} by histamine was abolished by 10 μM ranitidine, but not by 0.3 μM chlorpheniramine or 1 μM thiperamide (Fig. 2B).

Receptor binding assay with microsomal preparations from neonatal atria revealed the presence of binding sites for both the H_1 antagonist mepyramine and the H_2 receptor antagonist tiotidine. The maximum binding capacity (B_{max}) and dissociation constant (K_d) for mepyramine were 177.2±6.2 fmol/mg protein and 0.49±0.06, respectively ($n=4$), and those for tiotidine were 93.1±11.3 fmol/mg protein and 14.8±6.8, respectively ($n=4$).

DISCUSSION

The positive inotropic effect of histamine in neonatal guinea-pig left atria was antagonized by ranitidine (Fig. 1A). The observed pA_2 value of 6.46 was close to the reported pA_2 value of ranitidine against H_2 receptors in human atria.[16] In contrast, neither the H_1 antagonist chlorpheniramine nor the H_3 receptor antagonist thioperamide affected the positive inotropic effect. These results indicate that the positive inotropic effect of histamine on neonatal left atria is mediated by H_2 receptors. It is generally known that stimulation of H_2 receptors induces physiological responses through increase in cAMP concentration. The present result that the histamine-induced positive inotropy was enhanced by IBMX (Fig. 1B) suggests that this is the case with neonatal guinea-pig left atria.

Histamine prolonged the action potential duration in neonatal left atria through stimulation of H_2 receptors (Fig.

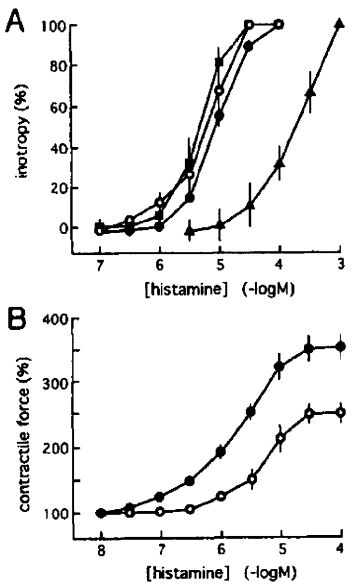

Fig. 1. Effects of Pharmacological Agents on the Histamine-Induced Positive Inotropy in Neonatal Guinea-Pig Left Atria

(A) Concentration–response relationship of histamine in the absence (open circles) and presence of receptor antagonists chlorpheniramine (0.3 μM; closed circles), ranitidine (10 μM; closed triangles) and thioperamide (1 μM, closed squares). Increase in contractile force after addition of each concentration was expressed as a percentage of the maximum increase. (B) Effect of isobutylmethylxantine (1 μM). Increase in contractile force after addition of each concentration was expressed as a percentage of the basal contractile force. Data points and vertical bars in A and B represent the mean±S.E.M. from 5 experiments

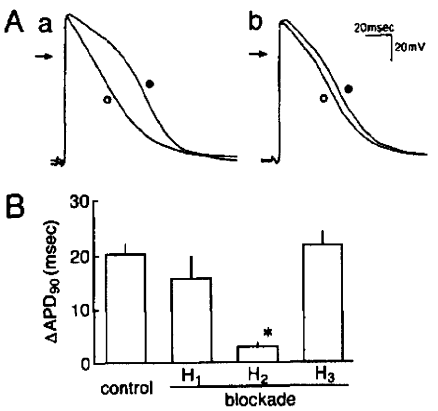

Fig. 2. Effect of Histamine on the Action Potential of Neonatal Guinea-Pig Left Atria

(A) Typical action potential records obtained before (open circles) and after (closed circles) the addition of histamine (10 μM) in the absence (a) and presence (b) of ranitidine (10 μM). Arrows indicate zero mV level. (B) Summarized results of the prolongation of action potential duration at 90% repolarization (APD_{90}). Columns and vertical bars represent the mean±S.E.M. from 5 experiments. The asterisks indicate statistical significance against the control value.

2). Such prolongation was also observed in adult left atria. The prolongation was mediated through H_1 receptors and inhibition of outward currents.[11,12] As the action potential properties of the guinea pig myocardium changes during postnatal development,[14,17] the ionic mechanisms, as well as the receptor type, for prolongation of the action potential by histamine may be different between the adult and neonatal left atria.

Receptor binding assay revealed the presence of both H_1 and H_2 receptors in the neonatal left atria. This means that, although two types of receptors are present, only the H_2 receptor is coupled to mechanisms leading to positive inotropy. In the adult left atria, both H_1 and H_2 receptors are present but only the H_1 receptor is coupled to positive inotropy. Thus, the receptors responsible for the histamine-induced inotropy change from H_2 to H_1 during postnatal development. Various properties in the excitation and contraction, as well as in the signal transduction mechanisms occur during myocardial development.[8] The intracellular mechanisms underlying the developmental shift from H_2 receptor-mediated to H_1 receptor-mediated inotropy in the guinea-pig left atria await further investigation. While it is established that H_2 receptor stimulation results in increased cAMP production, evidence both for[18] and against[19] the role of phosphoinositide hydrolysis in response to H_1 receptor stimulation has been reported. Clarification of the precise mechanisms for the H_1 receptor-mediated inotropy, as well as the developmental shift from H_2 to H_1, would contribute to the understanding of signal transduction mechanisms. Diminution of H_2 receptor-mediated inotropy was also reported in the developing chick ventricular myocardium.[20]

In conclusion, the present study revealed that the receptor type mediating the positive inotropy in the guinea-pig left atrial myocardium is converted from H_2 to H_1 during postnatal development. The present findings imply that the histamine-mediated mechanisms in the myocardium may change during postnatal development.

Acknowledgments This study was supported in part by the Science Research Promotion Fund from the Promotion and Mutual Aid Corporation for Private Schools of Japan (for YT and HT). This study was partly performed as a part of the project "Research on the molecular mechanisms of appearance of age-related diseases by failure of cell function control system, and their prevention and treatment" by the "Research Center for Aging and Age-Related Diseases" established in the Toho University Faculty of Pharmaceutical Sciences.

REFERENCES

1) McNeill J. H., *Can. J. Physiol. Pharmacol.*, **62**, 720—726 (1984).
2) Wolff A. A., Levi R., *Circ. Res.*, **58**, 1—16 (1986).
3) Hattori Y., *Methods Find. Exp. Clin. Pharmacol.*, **21**, 123—131 (1999).
4) Matsuda N., Hattori Y., Sakuraya F., Kobayashi M., Zhang X.-H., Kemmotsu O., Gando S., *Naunyn-Schmied. Arch. Pharmacol.*, **366**, 513—521 (2002).
5) Laher I. E., McNeill J. H., *Can. J. Physiol. Pharmacol.*, **58**, 1256—1261 (1980).
6) Tanaka H., Uesato N., Shigenobu K., *Naunyn-Schmied. Arch. Pharmacol.*, **352**, 626—630 (1995).
7) Endoh M., *J. Pharmacol. Sci.*, **100**, 525—537 (2006).
8) Tanaka H., Namekata I., Nouchi H., Shigenobu K., Kawanishi T., Takahara A., *J. Pharmacol. Sci.*, **109**, 327—333 (2009).
9) Levi R., Allan G., Zavecz J. H., *Fed. Proc. Fed. Am. Soc. Exp. Biol.*, **35**, 1942—1947 (1976).
10) Verma S. C., McNeill J. H., *J. Pharmacol. Exp. Ther.*, **200**, 352—362 (1977).
11) Hattori Y., Endou M., Gando S., Kanno M., *Br. J. Pharmacol.*, **103**, 1573—1579 (1991).
12) Yoshimoto K., Hattori Y., Houzen H., Kanno M., Yasuda K., *Br. J. Pharmacol.*, **124**, 1774—1750 (1998).
13) Shigenobu K., Sawada K., Kasuya Y., *Can. J. Physiol. Pharmacol.*, **58**, 1300—1306 (1980).
14) Agata N., Tanaka H., Shigenobu K., *Acta Physiol. Scand.*, **149**, 331—337 (1993).
15) Agata N., Tanaka H., Shigenobu K., *Eur. J. Pharmacol.*, **260**, 47—55 (1994).
16) Poli E., Medici D., Contini G. A., Bertaccini G., *Arch. Int. Pharmacodyn. Ther.*, **273**, 221—225 (1985).
17) Kato Y., Tanaka H., Shigenobu K., *J. Mol. Cell. Cardiol.*, **28**, 1515—1522 (1996).
18) Sakuma I., Gross S. S., Levi R., *J. Pharmacol. Exp. Ther.*, **247**, 466—472 (1988).
19) Hattori Y., Endou M., Shirota M., Kanno M., *Naunyn-Schmied. Arch. Pharmacol.*, **340**, 196—203 (1989).
20) Tanaka H., Uesato N., Shigenobu K., *Naunyn-Schmied. Arch. Pharmacol.*, **351**, 391—357 (1995).

Biochemical and Biophysical Research Communications 398 (2010) 284–289

Contents lists available at ScienceDirect

Biochemical and Biophysical Research Communications

journal homepage: www.elsevier.com/locate/ybbrc

Role of transient receptor potential vanilloid 2 in LPS-induced cytokine production in macrophages

Kenji Yamashiro [a,b,c], Tetsuo Sasano [d], Katsuyoshi Tojo [a], Iyuki Namekata [f], Junko Kurokawa [b], Naoki Sawada [c,d], Takayoshi Suganami [c], Yasutomi Kamei [c], Hikaru Tanaka [f], Naoko Tajima [a], Kazunori Utsunomiya [a], Yoshihiro Ogawa [c,e,*], Tetsushi Furukawa [b,**]

[a] Division of Diabetes and Endocrinology, Department of Internal Medicine, Jikei University School of Medicine, 1-5-45 Yushima, Bunkyo-ku, Tokyo 113-8510, Japan
[b] Department of Bio-informational Pharmacology, 1-5-45 Yushima, Bunkyo-ku, Tokyo 113-8510, Japan
[c] Department of Molecular Medicine and Metabolism, 1-5-45 Yushima, Bunkyo-ku, Tokyo 113-8510, Japan
[d] Medical Top Track Program, 1-5-45 Yushima, Bunkyo-ku, Tokyo 113-8510, Japan
[e] Global Center of Excellence Program, International Research Center for Molecular Science in Tooth and Bone Diseases, Medical Research Institute, Tokyo Medical and Dental University, 1-5-45 Yushima, Bunkyo-ku, Tokyo 113-8510, Japan
[f] Department of Pharmacology, Toho University Faculty of Pharmaceutical Sciences, 1-5-45 Yushima, Bunkyo-ku, Tokyo 113-8510, Japan

ARTICLE INFO

Article history:
Received 2 June 2010
Available online 23 June 2010

Keywords:
Transient receptor potential vanilloid 2
Macrophage
LPS
Cytokine
Calcium

ABSTRACT

There is considerable evidence indicating that intracellular Ca^{2+} participates as a second messenger in TLR4-dependent signaling. However, how intracellular free Ca^{2+} concentrations ($[Ca^{2+}]_i$) is increased in response to LPS and how they affect cytokine production are poorly understood. Here we examined the role of transient receptor potential (TRP), a major Ca^{2+} permeation pathway in non-excitable cells, in the LPS-induced cytokine production in macrophages. Pharmacologic experiments suggested that TRPV family members, but neither TRPC nor TRPM family members, are involved in the LPS-induced TNFα and IL-6 production in RAW264 macrophages. RT-PCR and immunoblot analyses showed that TRPV2 is the sole member of TRPV family expressed in macrophages. ShRNA against TRPV2 inhibited the LPS-induced TNFα and IL-6 production as well as IκBα degradation. Experiments using BAPTA/AM and EGTA, and Ca^{2+} imaging suggested that the LPS-induced increase in $[Ca^{2+}]_i$ involves both the TRPV2-mediated intracellular and extracellular Ca^{2+} mobilizations. BAPTA/AM abolished LPS-induced TNFα and IL-6 production, while EGTA only partially suppressed LPS-induced IL-6 production, but not TNFα production. These data indicate that TRPV2 is involved in the LPS-induced Ca^{2+} mobilization from intracellular Ca^{2+} store and extracellular Ca^{2+}. In addition to Ca^{2+} mobilization through the IP_3-receptor, TRPV2-mediated intracellular Ca^{2+} mobilization is involved in NFκB-dependent TNFα and IL-6 expression, while extracellular Ca^{2+} entry is involved in NFκB-independent IL-6 production.

1. Introduction

Macrophages are a central player of innate immunity and inflammation. They are capable of producing a variety of proinflammatory cytokines such as TNFα and IL-6 following Lps stimulation [1,2]. Intracellular signaling pathways downstream of TLR4 stimulation by LPS have been extensively studied [1,2]. Upon LPS stimulation, TLR4 initiates a series of NFκB- and MAPK-associated intracellular signaling events, thereby inducing the expression of an array of proinflammatory cytokine genes.

Intracellular free Ca^{2+} concentrations ($[Ca^{2+}]_i$) or Ca^{2+} fluxes are important for cellular responses to extracellular stimuli [3,4]. There is considerable evidence that intracellular Ca^{2+} participates as a second messenger in TLR4-dependent signaling [5]. Indeed, treatment with LPS causes a transient increase in $[Ca^{2+}]_i$, which is required for increased TNFα production in macrophages [6]. However, the molecular mechanisms by which LPS increases $[Ca^{2+}]_i$ and how the LPS-induced Ca^{2+} fluxes modulates proinflammatory cytokine production are still poorly understood.

Transient receptor potential (TRP) channels are a group of Ca^{2+}-permeable channels with diverse activation properties including temperature, pH changes, ADP-ribose, and diacylglycerol [7]. TRP channels are suggested to be an important Ca^{2+} entry pathway in non-excitable cells [7]. For instance, TRP vanilloid 4 (TRPV4)- and TRPV5-mediated Ca^{2+} influx is essential for terminal differentiation of osteoclasts and osteoclastic bone resorption [8,9]. Activation of the TRP melastatin 8 (TRPM8) variant in human lung epithelial cells also leads to increased expression of several cytokine and chemokine genes [10]. TRPV1 is expressed primarily in sensory nerves

* Corresponding author. Fax: +81 3 5803 4931.
** Corresponding author. Fax: +81 3 5803 4950.
E-mail addresses: ogawa.mmm@mri.tmd.ac.jp (Y. Ogawa), t_furukawa.bip@mri.tmd.ac.jp (T. Furukawa).

0006-291X/$ - see front matter © 2010 Elsevier Inc. All rights reserved.
doi:10.1016/j.bbrc.2010.06.082

and protects against the onset of LPS-induced sepsis [11]. Reactive oxygen species-induced chemokine production has been shown to be mediated through TRPM2-mediated Ca^{2+} influx in monocytes/macrophages [12]. However, whether TRP channels are involved in the LPS-induced Ca^{2+} mobilization in macrophages has not been addressed.

TRPV2 is a Ca^{2+} permeable channel originally identified in rat brain and human myeloid cell line, CCRF-CEM [13]. Here we provide *in vitro* evidence that TRPV2 is involved in LPS-induced Ca^{2+} mobilization and induction of cytokines in RAW macrophages. Our data will also help elucidate the molecular mechanisms underlying the LPS-induced cytokine production in macrophages and thus identify the therapeutic targets that may prevent or treat a variety of acute and chronic inflammatory diseases.

2. Materials and methods

2.1. Reagents

All reagents were purchased from Sigma–Aldrich (St. Louis, MO) or Nacalai Tesque (Kyoto, Japan). Rabbit mAbs against IκBα, and phospho-IκBα (Ser32) (p-IκBα) were purchased from Cell Signaling (Beverly, MA), and a rabbit polyclonal Ab against mouse TRPV2 (mTRPV2) from Abcam Inc. (Cambridge, MA).

2.2. Cell culture and transfection

A macrophages cell line RAW264 (RIKEN BioResource Center, Tsukuba, Japan), and HEK293T were maintained in DMEM (Nacalai Tesque, Kyoto, Japan) containing 10% FBS (BioWest, Miami, FL). To produce HEK293T cells expressing TRPV2, pcMV6-Kan/Neo-mTRPV2 (OriGene Technologies, RockVille, MD) was transfected by Lipofectamine™2000 (Invitrogen Life Technologies, CA). Murine bone marrow-derived macrophages were prepared as described [14].

2.3. Lentivirus short hairpin RNA (shRNA) vector construction and gene transduction

The construction of the shRNA for TRPV2 (NM_011706), and gene transduction were carried out as previously reported [15]. The sense and antisense oligonucleotides used are shown in Supplementary Table 1. Lentivirus-infected cells were detected as GFP-positive. After 4 weeks of selection, over 90% of cells were GFP-positive and used for further analysis.

2.4. Quantitative real-time RT-PCR analysis

Quantitative real-time RT-PCR was performed with SYBR Green PCR Master MixReagent Kit (Applied Biosystems, Foster City, CA) [16]. The primer sets used to detect each of TRPV members are shown in Supplementary Table 2.

2.5. Measurement of TNFα and IL-6 protein levels in culture media

The TNFα and IL-6 protein levels were determined by the commercially available enzyme-linked immunosorbent assay (ELISA) kits (R&D systems, Minneapolis, MN).

2.6. Immunoblot analysis

Immunoblot analysis was performed as described [16]. Membranes were immunoblotted with one of following primary Abs; p-IκBα (1:1000), IκBα (1:2000), α-tubulin (1:16,000), or mTRPV2 (1:500).

2.7. Measurement of $[Ca^{2+}]_i$ concentration

Measurement of $[Ca^{2+}]_i$ was performed with epifluorescent microscopy (Hamamatsu Photonics, Hamamatsu, Japan) as previously described [17]. Calibration between fluorescence ratio and Ca^{2+} concentration was performed *in situ* as described [18].

2.8. Statistical analysis

Data are expressed as the mean ± SEM. Statistical analysis was performed using Student's *t*-test. $P < 0.05$ was considered to be statistically significant.

3. Results

3.1. Effect of TRP channel blockers on the LPS-induced cytokine production in RAW264 and murine macrophages

Macrophages express several TRP channels including TRPC, TRPM, and TRPV family members [12,19]. To explore if TRP family members play a role in the LPS-induced inflammatory response, and if so, which TRP channel(s) are involved, we first used ruthenium red (RR), a non-selective TRP channel blocker [20], Gadolinium (Gd), a TRPC channel blocker at a low concentration (30 μM) and a TRPC and a TRPV channel blocker at a high concentration (1 mM) [20,21], and flufenamic acid (FFA), a TRPC and TRPM channel blocker [21,22]. Treatment with LPS at a dose of 5 ng/ml significantly increased TNFα and IL-6 mRNA expression ($P < 0.01$), which was markedly inhibited by RR (10 μM) (Fig. 1A). Treatment with Gd at a dose of 30 μM did not affect the LPS-induced TNFα and IL-6 mRNA expression (Fig. 1B), but, at a dose of 1 mM, it significantly inhibited the LPS-induced IL-6 mRNA expression ($P < 0.01$), but not TNFα mRNA expression (Fig. 1C). FFA (100 μM) did not affect the LPS-induced TNFα and IL-6 mRNA expression (Fig. 1D). Similarly, treatment with RR (10 μM) significantly suppressed the LPS-induced TNFα and IL-6 secretion ($P < 0.01$), while treatment with Gd at 1 mM inhibited the LPS-induced IL-6 secretion ($P < 0.01$), but not TNFα secretion (Supplementary Fig. 1).

We also examined effects of RR and Gd on the LPS-induced cytokine secretion from murine bone marrow-derived macrophages. RR (10 μM) significantly suppressed the TNFα and IL-6 secretion stimulated by LPS (10 ng/ml) for 6 h and 24 h ($P < 0.01$) (Fig. 1E). Gd (1 mM) suppressed IL-6 ($P < 0.05$), but not TNFα, secretion stimulated by LPS for 24 h (Fig. 1F).

These observations suggest that TRPV family members, but neither TRPC nor TRPM, are involved in the LPS-induced TNFα and IL-6 production in macrophages. Since the effects of RR and Gd are more prominent in RAW264, we used RAW264 in the following experiments.

3.2. Expression of TRPV2 in RAW264 macrophages

We examined expression of mRNAs for TRPV family members (TRPV1~6) in RAW264 macrophages. RT-PCR analysis revealed that TRPV2 mRNA is expressed in RAW264 macrophages (Fig. 2A). There were no appreciable amounts of mRNAs for TRPV1, 3, 4, 5, and 6. We examined TRPV2 protein expression in RAW264 macrophages. Immunoblot analysis identified two immunoreactive bands at ~110 and at ~85 kD (Fig. 2B), which may be the products of post-translational modification such as glycosylation and phosphorylation [23]. Expression of TRPV2 protein in RAW264 macrophages was further confirmed by the positive immune-staining with an anti-TRPV2 antibody in immune-cytochemical studies (Supplementary Fig. 2).

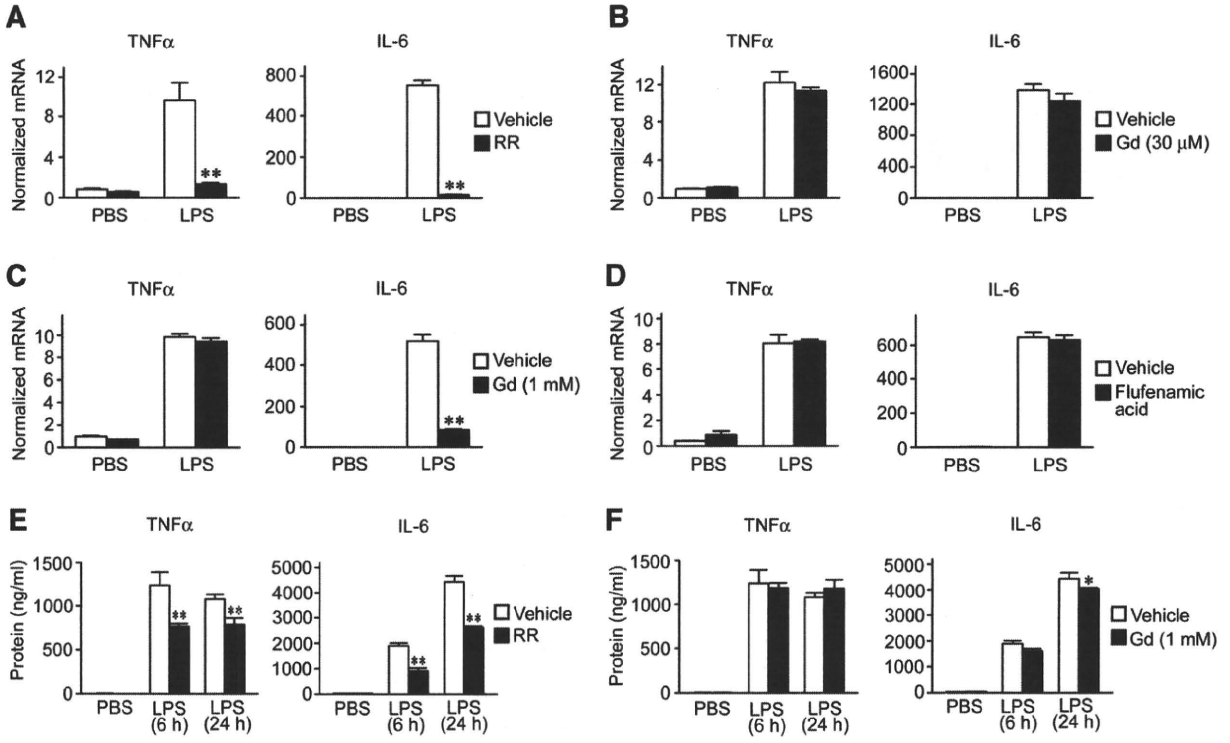

Fig. 1. Effect of TRP channel blockers on the LPS-stimulated cytokine mRNA expression in RAW264 macrophages and cytokine protein secretion from murine bone marrow macrophages. (A–D) Effect of pretreatments with RR at 10 μM (panel A), Gd at 30 μM (panel B), Gd at 1 mM (panel C), and flufenamic acid at 100 μM (panel D) on the LPS-induced TNFα (left panel) and IL-6 (right panel) mRNA expression. In this and following figures, data for mRNA expression were normalized to the value for 36B4 as an internal control, and expressed relative to the control value (vehicle application and no LPS stimulation). LPS; 5 ng/ml for 4 h. Data are mean of 4 experiments. *: $P < 0.05$, **: $P < 0.01$. E, F, Effect of pretreatments with RR at 10 μM (panel F) and Gd at 1 mM (panel G) on the LPS-induced TNFα (left panel) and IL-6 (right panel) protein secretion. LPS; 10 ng/ml for 6 h and 24 h. Data are mean of 4 experiments. *: $P < 0.05$, **: $P < 0.01$.

3.3. Effect of TRPV2 knock-down on the LPS-induced cytokine mRNA expression

To specifically address the role of TRPV2 in the LPS-induced TNFα and IL-6 production, we used the knock-down strategy with shRNA against TRPV2. RT-PCR and immunoblot analysis confirmed that both TRPV2 mRNA and protein levels are reduced in RAW264 macrophages transfected with shRNA for TRPV2 (V2KD-RAW macrophages), but not in those with scramble RNA (Scr-RAW macrophages) (Fig. 2C and D). Similar to wild-type RAW264 macrophages, LPS treatment (10 ng/ml) significantly increased TNFα and IL-6 mRNA expression in Scr-RAW macrophages ($P < 0.01$). In V2KD-RAW macrophages, the LPS-induced TNFα and IL-6 expression was significantly reduced (Fig. 2E). Collectively, these observations suggest that TRPV2 is crucially involved in the LPS-induced TNFα and IL-6 production in macrophages.

3.4. Role of TRPV2 in NFκB signaling pathway

We next examined the role of TRPV2 in NFκB signaling pathway, since it is the major pathway for LPS-induced cytokine production. Treatment with LPS-induced degradation of IκBα, which persisted for 60 min. Knock-down of TRPV2 significantly inhibited IκBα degradation (Fig. 3A and B). Treatment with RR (10 μM) abolished IκBα degradation, whereas Gd (1 mM) had no effect (Fig. 3A and B).

3.5. Role of TRPV2 on the LPS-induced $[Ca^{2+}]_i$ mobilization

We measured changes in $[Ca^{2+}]_i$ with a Ca^{2+} indicator Fura-2 to examine if TRPV2 is indeed involved in the LPS-induced intracellular Ca^{2+} mobilization. Treatment of RAW264 macrophages with LPS (5 ng/ml) induced a significant increase in $[Ca^{2+}]_i$ from 168 ± 26 nM to 661 ± 60 nM in 40 min ($n = 19$, $P < 0.01$). In V2KD-RAW macrophages, but not in Scr-RAW macrophages, the LPS-induced increase in $[Ca^{2+}]_i$ was suppressed (Fig. 4A). We also examined the effects of a TRPV2 channel blockers. RR (10 μM) and Gd (1 mM) significantly suppressed the LPS-induced increase in $[Ca^{2+}]_i$: from 142 ± 16 nM to 287 ± 23 nM for RR ($n = 18$, $P < 0.01$), and 135 ± 12 nM to 225 ± 14 nM for Gd ($n = 19$, $P < 0.01$) (Fig. 4A).

3.6. Role of Ca^{2+} mobilization in cytokine induction and IκBα degradation

To explore the role of Ca^{2+} mobilization in cytokine production, we first used BAPTA/AM and EGTA. When BAPTA/AM permeates into the cell, it is converted to BAPTA by intracellular esterase, and BAPTA chelates intracellular Ca^{2+}, while EGTA cannot permeate through the plasma membrane, thereby chelating extracellular Ca^{2+}. Intracellular Ca^{2+} removal by BAPTA suppressed the LPS-induced TNFα and IL-6 mRNA expression (Fig. 4B). On the other hand, pre-incubation with EGTA had no effect on TNFα mRNA expression, but partially suppressed IL-6 mRNA expression ($P < 0.01$) (Fig. 4C). We also examined the involvement of intracellular Ca^{2+} mobilization through ryanodine receptor and IP_3 receptor in the LPS-induced cytokine mRNA expression. In this study, dantrolene (30 μM), a ryanodine receptor inhibitor, did not inhibit the LPS-induced TNFα or IL-6 mRNA expression (Fig. 4D). On the other hand, Xestospondin C (20 μM), an IP_3 receptor inhibitor, partially inhibited the TNFα mRNA induction, and almost completely inhibited the IL-6 mRNA induction (Fig. 4E).

BAPTA/AM treatment markedly suppressed LPS-induced IκBα degradation, while EGTA had no effect (Supplementary Fig. 3).

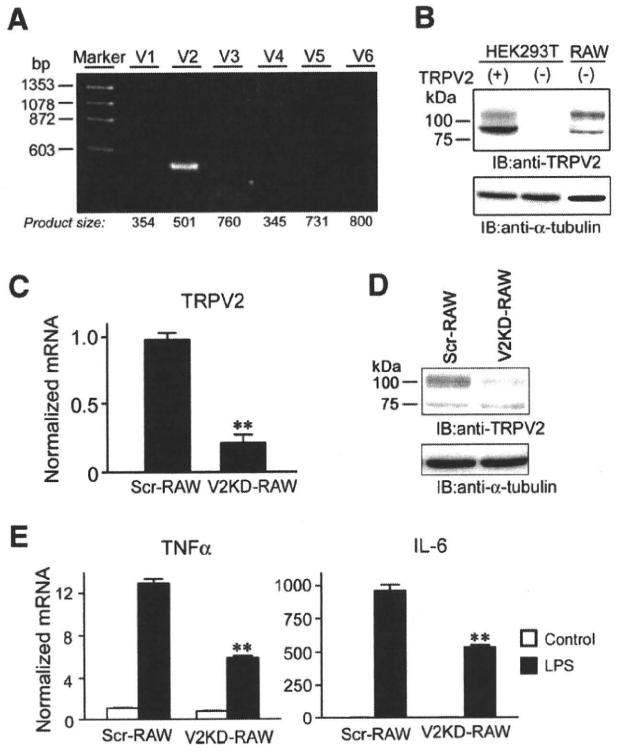

Fig. 2. Expression of TRPV channels and effects of TRPV2 knock-down on the LPS-stimulated cytokine mRNA production in RAW264. (A) Expression of mRNA for TRPV1~6 channels in RAW264 macrophages was analyzed with RT-PCR. (B) Expression of TRPV2 protein in RAW264 macrophages was examined with Western blot analysis. Left 2 lanes are data for HEK293T cells transfected with or without mTRPV2. (C) Effect of infection with lentivirus-scramble RNA (Scr-RAW) or lentivirus-shTRPV2 (V2KD-RAW) on TRPV2 mRNA expression in RAW264 macrophages. **: $P < 0.01$. (D) Effect of infection of lentivirus-scramble RNA (Scr-RAW) or lentivirus-shTRPV2 (V2KD-RAW) on TRPV2 protein expression in RAW264 macrophages. (E) Effect of TRPV2 knock-down on the LPS-induced cytokine mRNA expression. LPS; 10 ng/ml for 4 h. Data are mean of 4 experiments. *: $P < 0.05$, **: $P < 0.01$.

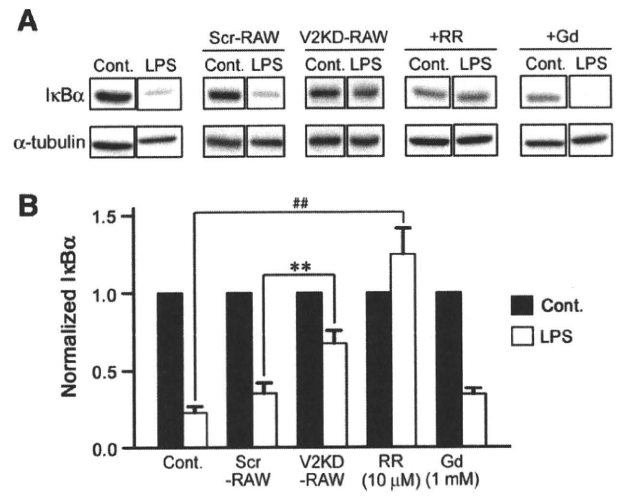

Fig. 3. Effect of TRPV2 knock-down and blockers on the LPS-induced IκBα degradation. (A) Representative data of Western blot analysis against IκBα, and α-tubulin as an internal control. Data were obtained just before (0 min) and 60 min after LPS treatment (5 ng/ml). (B) Densitometric analysis of 4–5 experiments. Density values for IκBα were normalized by that for α-tubulin, and expressed as a relative to the value just before LPS treatment (0 min). **: $P < 0.01$ vs. Scr-RAW; ##: $P < 0.01$ vs. control.

4. Discussion

Macrophages are capable of producing a variety of proinflammatory cytokines such as TNFα and IL-6 [2]. Upon Lps stimulation, TLR4 initiates a series of intracellular signaling pathways involving NFκB, thereby inducing an array of cytokine production [3,4]. Because LPS increases $[Ca^{2+}]_i$, which is shown to be required for increased cytokine production in macrophages [6,24], it is likely that intracellular Ca^{2+} participates as a second messenger in TLR4-dependent signaling [5,6]. However, how LPS increases $[Ca^{2+}]_i$ in macrophages are poorly understood. There is considerable evidence that TRP channels are an important Ca^{2+} entry pathway in non-excitable cells [7]. This study was, therefore, designed to elucidate the potential role of TRP channels in the LPS-induced Ca^{2+} fluxes and cytokine production in macrophages.

Pharmacologic experiments suggested that the LPS-induced TNFα and IL-6 production is markedly inhibited by RR, a non-selective TRP channel blocker. Moreover, treatment with Gd at the higher dose sufficient to block TRPV channels efficiently suppressed the LPS-induced IL-6 mRNA expression, which was unaffected at the lower dose. It is, therefore, likely that TRPV family members are involved in the LPS-induced TNFα and IL-6 production in macrophages. RT-PCR and immunoblot analyses revealed that TRPV2 mRNA and protein are expressed in RAW264 macrophages, where no appreciable amounts of mRNA for other TRPV family members are detected, which is consistent with previous reports [19,25]. Importantly, the LPS-induced TNFα expression and IL-6 expression were significantly reduced in V2KD-RAW246 macrophages relative to Scr-RAW macrophages. These observations suggest that TRPV2 is crucially involved in the LPS-induced TNFα and IL-6 production in macrophages.

Intracellular Ca^{2+} participates as a second messenger in TLR4-dependent signaling [5]; the LPS-induced transient increase in $[Ca^{2+}]_i$ is required for cytokine increase in macrophages [6]. Knock-down experiments suggest that TRPV2 is involved in LPS-induced $[Ca^{2+}]_i$ increase in RAW macrophages. BAPTA/AM chelates intracellular Ca^{2+}, while EGTA chelates extracellular Ca^{2+}. Treatment with BAPTA/AM abolishes both the LPS-induced TNFα and IL-6 production, while EGTA only inhibits the LPS-induced IL-6 production. BAPTA/AM inhibited LPS-induced IκBα degradation, EGTA had no effect on the LPS-induced IκBα degradation. A lipophilic compound RR can enter into the cell, and can inhibit TRPV2 localized intracellularly, while a cationic blocker Gd cannot permeate cell membrane and can inhibit TRPV2 localized on surface membrane. Thus, the data on BAPTA/AM and EGTA appear to be consistent with the finding that RR inhibits both TNFα and IL-6 production, while Gd only inhibits IL-6 production. Since RR, but not Gd, inhibited LPS-induced IκBα degradation, NFκB- and IκBα-dependent pathway may require intracellular Ca^{2+} mobilization, but not extracellular Ca^{2+} flux. Collectively, intracellular Ca^{2+} mobilization is crucial for NFκB-dependent TNFα and IL-6 expression, while extracellular Ca^{2+} entry is important in NFκB-independent IL-6 expression, and for both pathways, TRPV2 plays a role.

We also examined the involvement of 2 major intracellular Ca^{2+} mobilization pathways, ryanodine receptor and IP_3 receptor. In this study, a ryanodine receptor inhibitor dantrolene does not affect the LPS-induced TNFα or IL-6 mRNA expression. Thus, although RR is a potent inhibitor of ryanodine receptor [26], it is unlikely that ryanodine receptor contributes to the inhibitory effect of RR on the LPS-induced cytokine mRNA expression. In contrast, an IP_3 receptor inhibitor Xestospongin C partially inhibits the LPS-induced TNFα mRNA expression, and almost completely inhibits the LPS-induced IL-6 mRNA expression. Thus, intracellular Ca^{2+} mobilization through both IP_3 receptor and TRPV2 appears to play a role in the LPS-induced TNFα mRNA expression. Relative contribution of

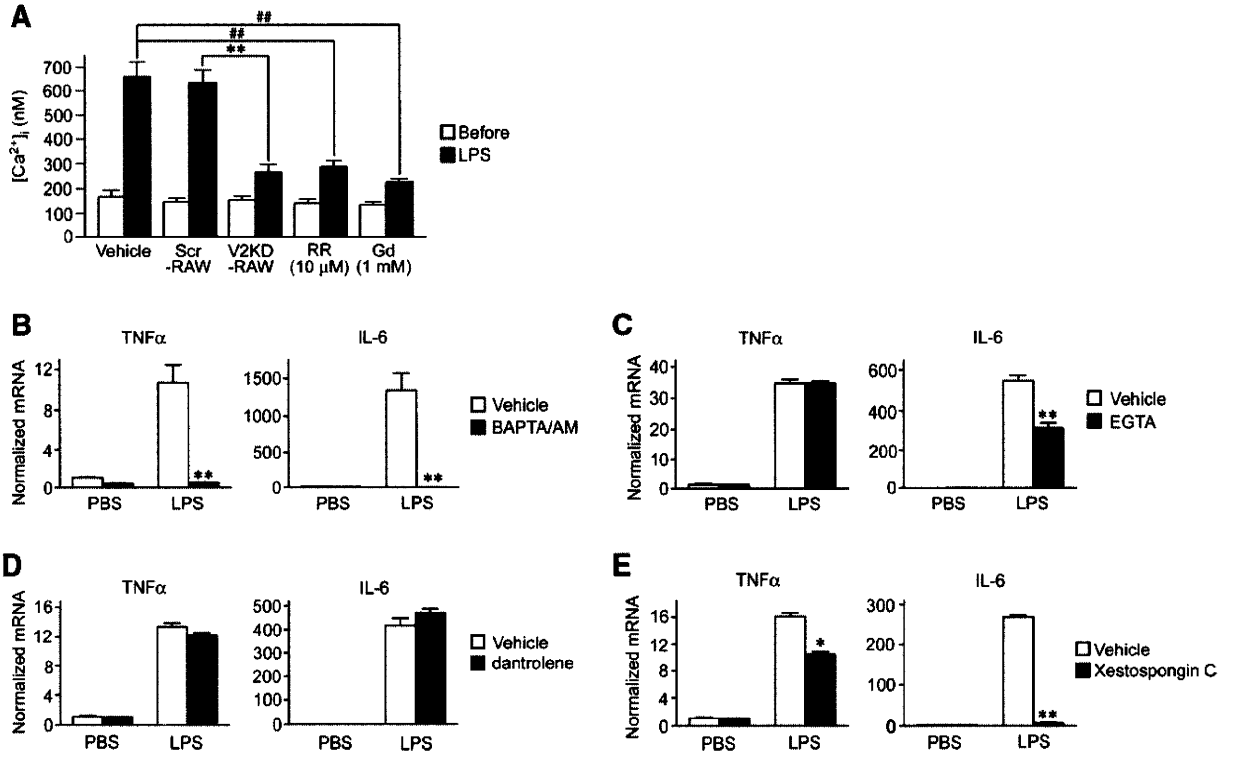

Fig. 4. Effect of shRNA and TRPV2 blockers on the LPS-induced in increase $[Ca^{2+}]_i$, and effect of Ca^{2+} removal and inhibition of intracellular Ca^{2+} mobilization on the LPS-induced cytokine mRNA expression A, $[Ca^{2+}]_i$ was measured with Ca^{2+} indicator Fura-2 before (filled bars) and 40 min (open bars) after LPS (5 ng/ml) application to RAW264 macrophages. Data are mean ± SEM of 18 or 19 experiments. **: $P < 0.01$ vs Scr-RAW; ##: $P < 0.01$ vs vehicle. B, C, D, E, Effects of removal of intracellular Ca^{2+} with BAPTA/AM (50 μM) (panel B), extracellular Ca^{2+} with EGTA (5 mM) (panel C), and inhibition of intracellular Ca^{2+} mobilization through a ryanodine receptor with dantrolene (30 μM) (panel D), and through an IP_3 receptor with Xestospongin C (20 μM) (panel E) on the LPS-induced TNFα (left panel) and IL-6 (right panel) mRNA expression. LPS; 5 ng/ml for 4 h. Data are mean of 4 experiments. *: $P < 0.05$, **: $P < 0.01$.

IP_3 receptor and TRPV2 to the LPS-induced TNFα mRNA expression and their relationship (additive or synergistic) remain unclear. In this study, BAPTA/AM and Xestospongin C completely inhibits the IL-6 mRNA induction, and EGTA and Gd partially inhibits it. These observations may imply that the LPS-induced IL-6 production is caused at least in part by Ca^{2+} mobilization solely from intracellular source and partly by entry of extracellular Ca^{2+} through TRPV2, which is triggered by intracellular Ca^{2+} mobilization through IP_3 receptor, a mechanism similar to the store-operated (SOC) or the receptor-operated Ca^{2+} entry (ROC) in TRPC channels [27,28]. The preliminary immune-cytochemical experiments confirm the presence of immune-positive staining both inside the cell and on the plasma membrane (Supplementary Fig. 2). Immuno-positive staining is present mainly inside the cell before Lps stimulation, and on the plasma membrane after LPS stimulation (Supplementary Fig. 2); however, the mechanism, kinetics, and implication of the TRPV2 transport are not addressed in this study and require further examination.

Recent paper using TRPV2 KO mice showed that TRPV2 has a pivotal role in macrophage particle binding and phagocytosis, without a significant role in inflammatory cytokine induction [29]. This effect was dependent on Na^+ influx through TRPV2, while in our experiments Ca^{2+} mobilization through TRPV2 appears to be crucial for LPS-induced cytokine induction. The different finding between their study and ours might be attributable to different experimental conditions: they stimulated murine peritoneal macrophages with LPS at 0.1 or 0.5 μg/ml for 24 h, while we stimulated RAW264 with LPS at 5 or 10 ng/ml for 4 h. To make experimental protocol comparable, we stimulated murine bone marrow-derived macrophages with LPS (10 ng/ml) for 6 and 24 h. Consistent with our experiments in RAW264 cells, RR suppressed TNFα and IL-6 secretion, and Gd (1 mM) suppressed IL-6 secretion. Thus, LPS may have different actions at low (5–10 ng/ml) and high (0.1–0.5 μg/ml) concentrations. To test this possibility, further studies are required.

5. Conclusion

This study represents the first demonstration that TRPV2 constitutes Ca^{2+} permeation pathways involved in the LPS-induced cytokine production in macrophages. Given the pathophysiologic role of TLR4 signaling [14,30], our data will also help identify the therapeutic targets that may prevent or treat a variety of inflammatory diseases.

Acknowledgments

We thank Dr. Itaru Kojima for primers used for RT-PCR and an Ab against TRPV2, and Dr. Hiroshi Nishina for critical reading of the manuscript. This work was supported in part by a Grant-in-Aid for Scientific Research from the Ministry of Education, Culture, Sports, Science and Technology of Japan (to T.F. and Y.O.), and a research grant from The Vehicle Racing Commemorative Foundation (to T.F.) and Takeda Science Foundation and The Naito Foundation (to Y.O.).

Appendix A. Supplementary data

Supplementary data associated with this article can be found, in the online version, at doi:10.1016/j.bbrc.2010.06.082.

References

[1] S. Akira, K. Takeda, Toll-like receptor signaling, Nat. Rev. Immunol. 4 (2004) 499–511.

[2] L.A.J. O'Neill, A.G. Bowie, The family of five: TIR-domain-containing adaptors in Toll-like receptor signaling, Nat. Rev. Immunol. 7 (2007) 353–364.

[3] A.J. Morris, C.C. Malbon, Physiological regulation of G protein-linked signaling, Physiol. Rev. 79 (1999) 1373–1430.

[4] M.D. Cahalan, H. Wulff, K.G. Chandy, Molecular properties and physiological roles of ion channels in the immune system, J. Clin. Immunol. 21 (2001) 235–252.

[5] X. Zhou, W. Yang, J. Li, Ca^{2+}- and protein kinase C-dependent signaling pathway for nuclear factor-kappa B activation, inducible nitric oxide synthase expression, and tumor necrosis factor-alpha production in lipopolysaccharide-stimulated rat peritoneal macrophages, J. Biol. Chem. 281 (2006) 31337–31347.

[6] S.N. Lichtman, J. Wang, C. Zhang, J.J. Lemasters, Endocytosis and Ca^{2+} are required for endotoxin-stimulated TNF-alpha release by rat Kupffer cells, Am. J. Physiol. 271 (1996) G920–G928.

[7] I.S. Ramsey, M. Delling, D.E. Clapham, An introduction to TRP channels, Ann. Rev. Physiol. 68 (2006) 619–647.

[8] R. Masuyama, J. Vriens, T. Voets, Y. Karashima, G. Owsianik, R. Vennekens, L. Lieben, S. Torrekens, K. Moermans, A.V. Bosch, R. Bouillon, B. Nilius, G. Carmeliet, TRPV4-mediated calcium influx regulates terminal differentiation of osteoclasts, Cell Metab. 8 (2008) 257–265.

[9] B.C.J. van der Eerden, J.G. J Hoenderop, T.J. de Vries, T. Schoenmaker, C.J. Buurman, A.G. Uitterlinden, H.A.P. Pols, R.J.M. Bindels, J.P.T.M. van Leeuwen, The epithelial Ca^{2+} channel TRPV5 is essential for proper osteoclastic bone resorption, Proc. Natl. Acad. Sci. USA 102 (2005) 17507–17512.

[10] A.S. Sabnis, C.A. Reilly, J.M. Veranth, G.S. Yost, Increased transcription of cytokine genes in human lung epithelial cells through activation of a TRPM8 variant by cold temperatures, Am. J. Physiol. 295 (2008) L194–L200.

[11] N. Clark, J. Keeble, E.S. Fernandes, A. Starr, L. Liang, D. Sugden, P. de Winter, S.D. Brain, The transient receptor potential vanilloid 1 (TRPV1) receptor protects against the onset of sepsis after endotoxin, FASEB J. 21 (2007) 3747–3755.

[12] S. Yamamoto, S. Shimizu, S. Kiyonaka, N. Takahashi, T. Wajima, Y. Hara, T. Negoro, T. Hiroi, Y. Kiuchi, T. Okada, S. Kaneko, I. Lange, A. Fleig, R. Penner, M. Nishi, H. Takeshima, Y. Mori, TRPM2-mediated Ca^{2+} influx induces chemokine production in monocytes that aggravates inflammatory neutrophil infiltration, Nat. Med. 14 (2008) 738–747.

[13] M.J. Caterina, T.A. Rosen, M. Tominaga, A.J. Brake, D. Julius, A capsaicin-receptor homologue with a high threshold for noxious heat, Nature 398 (1999) 411–436.

[14] T. Suganami, K. Tanimoto-Koyama, J. Nishida, M. Itoh, X. Yuan, S. Mizutani, H. Kotani, S. Yamaoka, K. Miyake, S. Aoe, Y. Kamei, Y. Ogawa, Role of the toll-like receptor 4/NF-kappaB pathway in saturated fatty acid-induced inflammatory changes in the interaction between adipocytes and macrophages, Arterioscler. Thromb. Vasc. Biol. 27 (2007) 84–91.

[15] E. Kizana, C.Y.S.L. Ginn, D.G. Allen, D.L. Ross, I.E. Alexander, Fibroblasts can be genetically modified to produce excitable cells capable of electrical coupling, Circulation 111 (2005) 394–398.

[16] R. Kouyama, T. Suganami, J. Nishida, M. Tanaka, T. Toyoda, M. Kiso, T. Chiwata, Y. Miyamoto, Y. Yoshimasa, A. Fukamizu, M. Horiuchi, Y. Hirata, Y. Ogawa, Attenuation of diet-Induced weight gain and adiposity through increased energy expenditure in mice lacking angiotensin II type 1a receptor, Endocrinology 146 (2005) 3481–3489.

[17] I. Namekata, T. Kawanishi, N. Iida-Tanaka, N. Tanaka, K. Shigenobu, Quantitative fluorescence measurement of cardiac Na^{+} /Ca^{2+} exchanger inhibition by kinetic analysis in stably transfected HEK293 cells, J. Pharmacol. Sci. 101 (2006) 356–360.

[18] H. Tanaka, T. Kawanishi, Y. Kato, R. Nakamura, K. Shigenobu, Restricted propagation of cytoplasmic Ca^{2+} oscillation into the nucleus in guinea pig cardiac myocytes as revealed by rapid scanning confocal microscopy and indo-1, Jpn. J. Pharmacol. 70 (1996) 235–242.

[19] M. Nagasawa, Y. Nakagawa, S. Tanaka, I. Kojima, Chemotactic peptide fMetLeuPhe induces translocation of the TRPV2 channel in macrophages, J. Cell. Physiol. 210 (2007) 692–702.

[20] M.J. Caterina, Transient receptor potential ion channels as participants in thermosensation and thermoregulation, Am. J. Physiol. 292 (2007) R64–R76.

[21] A.P. Albert, V. Pucovsky, S.A. Prestwich, W.A. Large, TRPC3 properties of a native constitutively active Ca^{2+} permeable cation channel in rabbit ear artery myocytes, J. Physiol. 571 (2006) 361–369.

[22] P. Massullo, A. Sumoza-Toledo, H. Bhagat, S. Partida-Sanchez, TRPM channels, calcium and redox sensors during innate immune responses, Semin. Cell. Dev. Biol. 17 (2006) 654–666.

[23] K. Boels, G. Glassmeier, D. Herrmann, I.B. Riedel, W. Hampe, I. Kojima, J.R. Schwarz, H.C. Schaller, The neuropeptide head activator induces activation and translocation of the growth-factor-regulated Ca^{2+} permeable channel GRC, J. Cell. Sci. 114 (2001) 3599–3606.

[24] O. Letari, S. Nicosia, C. Chiavaroli, P. Vacher, W. Schlegel, Activation by bacterial lipopolysaccharide causes changes in the cytosolic free calcium concentration in single peritoneal macrophages, J. Immunol. 147 (1991) 980–983.

[25] M. Kanzaki, Y.Q. Zhang, H. Mashima, L. Li, H. Shibata, I. Kojima, Translocation of a calcium-permeable cation channel induced by insulin-like growth factor-I, Nat. Cell. Biol. 1 (1999) 165–170.

[26] R. Zucchi, S. Ronca-Testoni S, The sarcoplasmic reticulum Ca^{2+} channel/ryanodine receptor: modulation by endogenous, effectors drugs and disease state, Pharmacol. Rev. 49 (1997) 1–51.

[27] L.-P. He, T. Hewavitharana, J. Soboloff, M.A. Spassova, D.L. Gill, A functional link between store-operated and TRPC channels revealed by the 3,5-bis(trifluoromethyl)pyrazole derivative, BTP2, J. Biol. Chem. 280 (2005) 10997–11006.

[28] S. Thebault, A. Zholos, A. Enfissi, C. Slomianny, E. Dewailly, M. Roudbarki, J. Parys, N. Prevarskaya, Receptor-operated Ca^{2+} entry mediated by TRPC3/TRPC6 proteins in rat prostate smooth muscle (PS1) cell line, J. Cell. Physiol. 204 (2005) 320–328.

[29] T.M. Link, U. Park, B.M. Vonakis, D.M. Raben, M.J. Soloski, M.J. Caterina, TRPV2 has a pivotal role in macrophage particle binding and phagocytosis, Nat. Immunol. 11 (2010) 232–239.

[30] C. Leon, R. Tory, J. Jia, O. Sivak, K. Wasan, Discovery and development of Toll-like receptor 4 (TLR4) antagonists: a new paradigm for treating sepsis and other diseases, Pharm. Res. 25 (2008) 1751–1761.

Blocking Effect of NIP-142 on the KCNQ1/KCNE1 Channel Current Expressed in HEK293 Cells

Iyuki NAMEKATA,[a] Noriko TSURUOKA,[a] Yayoi TSUNEOKA,[a] Tomoyuki MATSUDA,[a,b] Akira TAKAHARA,[a] Yoshio TANAKA,[a,c] Takeshi SUZUKI,[a,d] Tetsuo TAKAHASHI,[e] Naoko IIDA-TANAKA,[a,f] and Hikaru TANAKA*,[a]

[a] *Department of Pharmacology, Faculty of Pharmaceutical Sciences, Toho University;* [c] *Department of Chemical Pharmacology, Faculty of Pharmaceutical Sciences, Toho University;* [c] *Department of Biophysical Chemistry, Faculty of Pharmaceutical Sciences, Toho University; Funabashi, Chiba 274–8510, Japan:* [b] *Biological Research Laboratories, Nissan Chemical Industries, Ltd.; Shiraoka, Saitama 349–0294, Japan:* [d] *School of Material Science, Japan Advanced Institute of Science and Technology; Tatsunokuchi, Ishikawa 923–1292, Japan: and* [f] *Department of Food Science, Otsuma Women's University; Chiyoda-ku, Tokyo 102–8357, Japan.*

Received September 14, 2010; accepted October 29, 2010; published online November 5, 2010

We examined the effect of NIP-142, a benzopyran compound with terminating effect on experimental atrial arrhythmia, on the KCNQ1/KCNE1 channel, which underlies the slow component of the cardiac delayed rectifier potassium channel (I_{Ks}). NIP-142, as well as chromanol 293B, showed concentration-dependent blockade of the current expressed in HEK293 cells; the EC_{50} value of NIP-142 and chromanol 293B for the inhibition of tail current was 13.2 μM and 4.9 μM, respectively. These results indicate that NIP-142 has blocking effect on the KCNQ1/KCNE1 channel current.

Key words NIP-142; KCNQ1; KCNE1; atrial fibrillation

Atrial fibrillation is one of the most frequent types of arrhythmia in clinical practice. It is reported to double the risk of deaths due to cardiovascular diseases and to be the major risk factor for thromboembolism, especially cerebral embolism.[1] At present, atrial fibrillation is mainly treated with class I antiarrhythmic agents such as pilsicainide and flecainide, or class III antiarrhythmic agents such as dofetilide and amiodarone,[2—4] but the major problem with these agents is that they also affect ventricular excitation and repolarization. Thus, drugs with atrial selectivity are desired for the treatment of atrial fibrillation.

NIP-142, (3*R**,4*S**)-4-cyclopropylamino-3,4-dihydro-2,2-dimethyl-6-(4-methoxyphenylacethylamino)-7-nitro-2*H*-1-benzopyran-3-ol, is a benzopyran derivative with terminating effects on canine vagal stimulation-induced atrial fibrillation model and on canine Y-shaped incision-induced atrial flutter model.[5—7] These effects have been attributed to prolongation of atrial refractory period. The prolongation of the refractory period and action potential duration (APD) by NIP-142 was observed in the atrium,[5,8] but not in the ventricle.[8] This may indicate that NIP-142 is less likely to disturb ventricular repolarization when applied for the treatment of atrial arrhythmia.

Concerning the molecular mechanisms for the action potential prolongation by NIP-142, blocking effects on potassium currents such as the acetylcholine-activated potassium current (I_{KACh})[8,9] and the ultrarapid component of the delayed rectifier potassium current (I_{Kur})[10] has been reported. The blocking effect on the rapid component of the delayed rectifier potassium current (I_{Kr}) was observed only at higher concentrations. The fast component (I_{Kr}) and the slow component (I_{Ks}) of the delayed rectifier potassium current are the two major currents responsible for atrial repolarization in species including the guinea-pig and human.[11] However, the effect of NIP-142 on I_{Ks} has not yet been reported. In the present study, we examined the effect of NIP-142 on currents through expressed potassium channel subunits KCNQ1/KCNE1, which underlie I_{Ks}.

MATERIALS AND METHODS

Preparation of HEK293 Cells Expressing Human KCNQ1/KCNE1 Channel Currents cDNA fragments for human KCNQ1 and KCNE1, which encode the two subunits of the I_{Ks} channel, were amplified by polymerase chain reaction from a human heart cDNA library (Takara Shuzo Co., Ltd., Kyoto, Japan) with oligonucleotide primers designed based on the published mouse cDNA sequence of KCNQ1 (GenBank accession number U89364) and KCNE1 (GenBank accession number NM000219), and assembled to obtain the full length cDNAs. They were inserted into the vector pIRES (Clontech, Palo Alto, CA, U.S.A.) to yield a tricistronic expression vector from which a single mRNA coding KCNQ1, KCNE1, and the neomycin resistance protein is transcribed. This vector, together with the vector pIRES-hrGFP-1α (Stratagene, Garden Grove, CA, U.S.A.), which encodes the green fluorescence protein (GFP), was introduced into HEK293 cells with lipofectamine (Invitrogen, Tokyo) and stable transformants were obtained by clone culture in the presence of G418 (500 μg/ml), a neomycin analog. Stable transformants of HEK293 cells expressing KCNQ1/KCNE1 channels were obtained as described in our previous report.[9] The cells expressing either channel were plated on glass coverslips 48 to 72 h before electrophysiological experiments.

Electrophysiological Recording of Expressed KCNQ1/KCNE1 Channel Current Whole-cell voltage clamp experiments were performed with HEK293 cells expressing KCNQ1/KCNE1 channels in a chamber mounted on the stage of an inverted microscope. The chamber was perfused continuously at a flow rate of 1.0 to 2.0 ml/min and the temperature was maintained at 22—25 °C. The external solution

* To whom correspondence should be addressed. e-mail: htanaka@phar.toho-u.ac.jp

was of the following composition: 128.0 mM NaCl, 20.0 mM KCl, 1.8 mM $CaCl_2$, 1 mM $MgCl_2$, 0.33 mM NaH_2PO_4, 5.0 mM *N*-(2-hydroxyethyl)piperazine-*N'*-2-ethanesulfonic acid (HEPES), 10.0 mM glucose (pH 7.4 with NaOH). The patch pipette solution was of the following composition: 100 mM KOH, 40 mM KCl, 70 mM aspartic acid, 1 mM $MgCl_2$, 5 mM ATP-K_2, 5 mM creatine phosphate-K_2, 5 mM HEPES, 10 mM ethylene glycol bis(2-aminoethylether)-*N,N,N',N'*-tetraacetic acid (EGTA) (pH 7.2 with KOH). Pipette tip resistances were 2 to 4 MΩ when filled with the patch pipette solution. The KCNQ1/KCNE1 channel current was measured as the amplitude of the peak tail current on return to a holding potential of −40 mV from 3 s voltage clamp pulses. Data acquisition and analyses were performed with the system described previously[9] including a patch-clamp amplifier (Axopatch 1D; Axon Instruments, Foster City, CA, U.S.A.), a personal computer (Prolinea 486; Compaq, Houston, TX, U.S.A.) and pCLAMP software (Axon).

Drugs and Chemicals NIP-142 was synthesized and provided by Nissan Chemical Industries (Tokyo, Japan). NIP-142 was added to the bath solution from a stock solution (100 mM) in 0.1 M HCl. The final concentration of HCl in the measuring bath (<0.1 mM) did not affect any of the experimental parameters measured. All other chemicals were commercial products of the highest available grade of quality.

RESULTS

In whole cell voltage clamped HEK293 cells expressing the KCNQ1/KCNE1 channel, depolarization to membrane potentials more positive than −10 mV induced voltage- and time-dependent outward currents. On repolarization to −40 mV, outward tail currents were observed (Figs. 1A, C). The peak amplitude of the tail current after a depolarizing pulse to 20 mV was 8.6±0.8 pA/pF (n=10).

Chromanol 293B, at 1 to 30 μM, concentration-dependently reduced the outward currents on depolarization and the tail currents on repolarization (Figs. 1A, B). The current density of the tail current after a depolarizing pulse to 20 mV in the absence and presence of 1, 3, 10 and 30 μM chromanol 293B was 7.5±1.4 pA/pF (n=10), 5.4±0.4 pA/pF (n=4), 4.5±0.9 pA/pF (n=5), 2.2±0.2 pA/pF (n=6) and 0.1±0.2 pA/pF (n=4), respectively. The EC_{50} value for the inhibition of tail current on repolarization from 20 mV was 4.9 μM (Fig. 1E).

NIP-142, at 10 and 30 μM, concentration-dependently reduced the outward currents on depolarization and the tail current on repolarization (Fig. 1C). The current density of the tail current after a depolarizing pulse to 20 mV in the absence and presence of 1, 10 and 30 μM NIP-142 was 9.7±0.7 pA/pF (n=10), 9.5±1.4 pA/pF (n=4), 5.4±1.0 pA/pF (n=5) and 1.8±0.5 pA/pF (n=5), respectively. The EC_{50} value for the inhibition of tail current on repolarization from 20 mV was 13.2 μM (Fig. 1E).

DISCUSSION

NIP-142 concentration-dependently blocked the KCNQ1/KCNE1 channel current with an EC_{50} value of 13.2 μM (Fig. 1). The reported EC_{50} value of NIP-142 for the GIRK1/4 channel current is 0.64 μM,[9] that for the Kv1.5

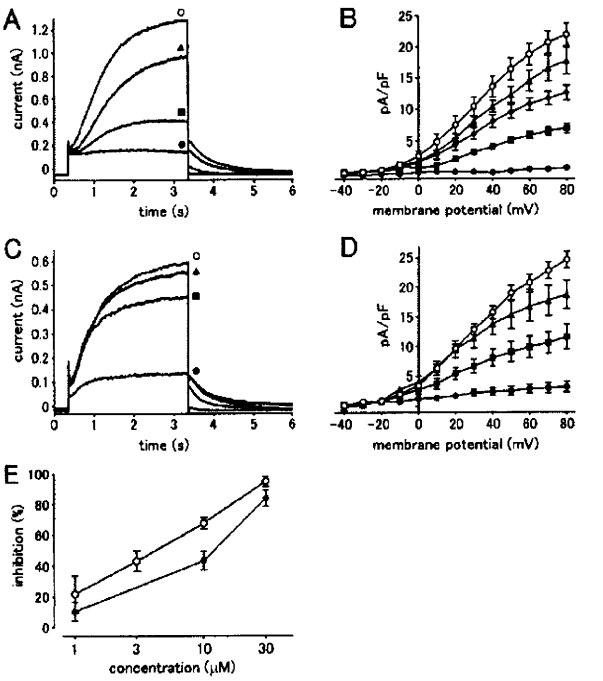

Fig. 1. Effect of Chromanol 293B and NIP-142 on KCNQ1/KCNE1 Channel Currents Expressed in HEK293 Cells

(A) Typical recordings in the absence (open circles) and presence of 1 μM (closed triangles), 10 μM (closed squares) and 30 μM (closed circles) chromanol 293B. (B) Summarized current–voltage relationships for the peak outward tail current on repolarization to −40 mV from a 3 s depolarization to various test potentials in the absence (open circles) and presence of 1 μM (closed triangles), 3 μM (closed diamonds), 10 μM (closed squares) and 30 μM (closed circles) chromanol 293B. (C) Typical recordings of the effects of NIP-142. (D) Summarized current–voltage relationships for the peak outward tail current on repolarization to −40 mV from a 3 s depolarization to various test potentials in the absence (open circles) and presence of 1 μM (closed triangles), 10 μM (closed squares) and 30 μM (closed circles) NIP-142. (E) Concentration–response relationship for blockade by chromanol 293B (open circles) and NIP-142 (closed circles) of the peak tail current on repolarization from 20 mV. Symbols and bars represent the mean±S.E.M from 4 to 8 experiments.

channel current is 4.8 μM,[10] and that for the HERG channel current is 44 μM.[9] The blocking potency of NIP-142 on the KCNQ1/KCNE1 channel current was relatively low, suggesting that the prolongation of atrial action potential by the compound is mainly produced by blockade of potassium currents other than I_{Ks}, especially the acetylcholine-activated potassium current. However, as the concentration range of NIP-142 (10 to 100 μM) to prolong the atrial action potential[8] overlaps that to inhibit the KCNQ1/KCNE1 channel current (Fig. 1E), the possibility that I_{Ks} blockade contributes to the effect of NIP-142 can not be totally excluded. The I_{Ks} current is known to be increased by factors such as β-adrenergic stimulation[12] or angiotensin II.[13] A gain-of-function mutation of KCNQ1 was reported to cause atrial fibrillation.[14] Development of novel I_{Ks} blockers with antiarrhythmic activity are in progress.[15] Thus, the I_{Ks}-blocking effect of NIP-142 may contribute to its antifibrillatory activity under certain pathological conditions.

NIP-142 was reported not to prolong the action potential duration in isolated guinea-pig ventricular tissue preparations,[8] despite its inhibitory effect on the KCNQ1/KCNE1 channel current. One explanation for this apparent discrepancy is the variation in sensitivity among experimental sys-

tems. There are cases in which potency of ion channel inhibitors are higher in voltage-clamped single cells than in myocardial tissue preparations (*S*(+)-Efonidipine[16]). The extent of I_{Ks}-blockade by NIP-142 in tissue preparations might be smaller than expected from the present results. Another possible explanation for the lack of action potential prolongation by NIP-142 in the ventricle is its blocking effect on calcium channels. We have observed that NIP-142 has blocking effect on the L-type calcium channel,[17] which may counteract its action potential-prolonging effect through potassium channel blockade. In any case, the details for the mechanisms of action of NIP-142 remain to be investigated.

Acknowledgments This study was supported in part by the Science Research Promotion Fund from the Promotion and Mutual Aid Corporation for Private Schools of Japan (for Y. Tanaka and H. Tanaka). This study was partly performed as a part of the project "Research on the molecular mechanisms of appearance of age-related diseases by failure of cell function control system, and their prevention and treatment" by the "Research Center for Aging and Age-Related Diseases" established in the Toho University Faculty of Pharmaceutical Sciences.

REFERENCES

1) Sugimoto T., Hayakawa K., Kasanuki H., "Atrial Fibrillation, Flutter, and Tachycardia," ed. by Hayakawa K., Kasanuki H., Igaku-Shoin, Tokyo, 1999, pp. 14—18.
2) Aliot E., Denjoy I., *Am. J. Cardiol.*, **77**, 66A—71A (1996).
3) Iwasaki H., Takahara A., Nakamura Y., Satoh Y., Nagai T., Shinkai N., Sugiyama A., *J. Pharmacol. Sci.*, **110**, 410—414 (2009).
4) Lenz T., Hilleman D., *Drugs Today* (Barc), **36**, 759—771 (2000).
5) Nagasawa H., Fujiki A., Fujikura N., Matsuda T., Yamashita T., Inoue H., *Circ. J.*, **66**, 185—191 (2002).
6) Tanaka H., Hashimoto N., *Cardiovas. Drug Rev.*, **25**, 342—356 (2007).
7) Hashimoto N., Tanaka H., "Progress in Cardiac Arrhythmia Research," ed. by Tarkowicz I. R., Nova Science Publishers, Hauppague, 2009, pp. 125—139.
8) Matsuda T., Takeda K., Ito M., Yamagishi R., Tamura M., Nakamura H., Tsuruoka N., Saito T., Masumiya H., Suzuki T., Iida-Tanaka N., Itokawa M., Yamashita T., Tsuruzoe N., Tanaka H., Shigenobu K., *J. Pharmacol. Sci.*, **98**, 33—40 (2005).
9) Matsuda T., Ito M., Ishimaru S., Tsuruoka N., Saito T., Iida-Tanaka N., Hashimoto N., Yamashita T., Tsuruzoe N., Tanaka H., Shigenobu K., *J. Pharmacol. Sci.*, **101**, 303—310 (2006).
10) Matsuda T., Masumiya H., Tanaka N., Yamashita T., Tsuruzoe N., Tanaka Y., Tanaka H., Shigenobu K., *Life Sci.*, **68**, 2017—2024 (2001).
11) Bosch R. F., Gaspo R., Busch A. E., Lang H. J., Li G. R., Nattel S., *Cardiovas. Res.*, **38**, 441—450 (1998).
12) Sanguinetti M. C., Jurkiewicz N. K., Scott A., Siegl K. S., *Circ. Res.*, **68**, 77—84 (1991).
13) Zankov D. P., Omatsu-Kanbe M., Isono T., Toyoda F., Ding W. G., Matsuura H., Horie M., *Circulation*, **113**, 1278—1286 (2006).
14) Chen Y. H., Xu S. J., Bendahhou S., Wang Y., Xu W. Y., Jin H. W., Sun H., Su X. Y., Zhuang Q. N., Yang Y. Q., Li Y. B., Liu Y., Xu H. J., Li X. F., Ma N., Mou C. P., Chen Z., Barhanin J., Huang W., *Science*, **299**, 251—254 (2003).
15) Salataa J. J., Scinickb H. G., Lynch J. J. Jr., *Curr. Med. Chem.*, **11**, 29—44 (2004).
16) Tanaka H., Namekata I., Ogawa T., Tsuneoka Y., Komikado C., Takahara A., Iida-Tanaka N., Izumi-Nakaseko H., Tsuru H., Adachi-Akahane S., *Eur. J. Pharmacol.*, **649**, 263—267 (2010).
17) Matsuda T., Masumiya H., Saito T., Tanaka H., Shigenobu K., *Jpn. J. Pharmacol.*, **79** (Suppl. I), 178P (1999).

J Pharmacol Sci 115, 235 – 238 (2011)

Journal of Pharmacological Sciences

Short Communication

Developmental Changes in Action Potential Prolongation by K^+-Channel Blockers in Chick Myocardium

Hideaki Nouchi[1], Naoaki Kiryu[1], Mikio Kimata[1], Yayoi Tsuneoka[1], Shogo Hamaguchi[1], Iyuki Namekata[1,*], Akira Takahara[1], Koki Shigenobu[1], and Hikaru Tanaka[1]

[1]*Department of Pharmacology, Toho University Faculty of Pharmaceutical Sciences, Miyama 2-2-1, Funabashi, Chiba 274-8510, Japan*

Received August 7, 2010; Accepted December 12, 2010

Abstract. The effects of K^+-channel blockers on the action potential duration of the myocardium were examined in isolated right ventricles from the 7 – 10-day-old, 11 – 13-day-old, and 14 – 20-day-old embryo and 1 – 7-day-old hatched chicks. E-4031 significantly prolonged action potential duration at all developmental stages examined; the prolongation was largest in the 11 – 13-day-old embryo and was accompanied by early after-depolarizations. Chromanol 293B showed smaller prolongation at all stages examined. Terfenadine prolonged action potential duration in the 11 – 13-day-old embryo, but not in other stages. Thus, the chick ventricular myocardium changes its repolarization properties during development.

Keywords: chick, K^+-channel blocker, action potential duration

The chick embryo heart has been used to study various aspects of myocardial excitation and contraction. Although the chick heart shares common basic mechanisms with the mammalian heart, characteristic features in the electrophysiological properties, Ca^{2+} handling, contraction, and their physiological and pharmacological regulation has been reported (1 – 4). Concerning its electrophysiological properties, the resting membrane potential and action potential amplitude was reported to increase progressively during embryonic development (1), and many reports have been published concerning the depolarizing membrane currents involved (2). On the other hand, relatively little is known about its repolarization process, which is the determinant of the action potential duration. In the case of mammalian myocardia, information on the species difference and developmental changes in repolarization properties have accumulated, which enables appropriate selection of preparations for different experimental purposes (4). In the present study, we intended to obtain information about the repolarization mechanisms of the chick heart. We applied standard microelectrode techniques to the chick embryonic ventricular myocardia from four different developmental stages and examined the effect of inhibitors of the delayed rectifier potassium current, the major repolarizing current in the myocardium.

Standard microelectrode experiments were performed as previously described (5 – 7). Briefly, fertilized chicken eggs were incubated at 37°C, and the right ventricular free wall was isolated from 7 – 10-day-old embryo, 11 – 13-day-old embryo, 14 – 20-day-old embryo, and 1 – 7-day-old hatched chicks. They were driven at 1 Hz in an organ bath containing physiological salt solution of the following composition: 118.4 mM NaCl, 4.7 mM KCl, 2.5 mM $CaCl_2$, 1.2 mM $MgCl_2$, 1.2 mM KH_2PO_4, 24.9 mM $NaHCO_3$, and 11.1 mM glucose. The solution was gassed with 95% O_2 – 5% CO_2 and maintained at 37°C (pH 7.4). All experimental data are expressed as the mean ± S.E.M., and statistical significance of differences between means were evaluated by the paired *t*-test. A P value less than 0.05 were considered significant. The drugs used were E-4031 (Wako, Osaka), chromanol 293B (Sigma, St. Louis, MO, USA), and terfenadine (Wako). All other drugs and chemicals were commercial products of the highest available quality.

The resting potential, overshoot and the maximum rate of rise increased progressively during the embryonic period (Table 1, Fig. 1A). Action potential duration increased progressively during the embryonic period. The action potential duration of 1 – 7-day-old hatched chicks

*Corresponding author. iyuki@phar.toho-u.ac.jp
Published online in J-STAGE on January 20, 2011 (in advance)
doi: 10.1254/jphs.10205SC

Table 1. Developmental changes in action potential parameters

Parameters (units)	7 – 10-day-old embryo	11 – 13-day-old embryo	14 – 20-day-old embryo	1 – 7-day-old hatched chicks
RP (mV)	−78.8 ± 0.3	−80.8 ± 0.4	−82.4 ± 0.3	−82.8 ± 0.3
OS (mV)	34.4 ± 0.5	36.7 ± 0.4	37.7 ± 0.5	37.3 ± 0.3
APD_{20} (ms)	103.1 ± 2.7	103.4 ± 2.8	106.9 ± 2.9	102.3 ± 2.7
APD_{50} (ms)	152.8 ± 3.0	154.3 ± 2.7	163.9 ± 2.6	145.5 ± 2.8
APD_{90} (ms)	180.4 ± 2.6	185.6 ± 2.6	197.8 ± 1.7	168.5 ± 2.8
$\dot{V}_{max}$ (V/s)	118.2 ± 6.3	149.3 ± 8.4	180.1 ± 4.1	177.8 ± 3.7

Action potential parameters of ventricular myocardia from 7 – 10-day-old embryos, 11 – 13-day-old embryos, 14 – 20-day-old embryos, and 1 – 7-day-old hatched chicks were obtained in the absence of agents. RP, OS, and $\dot{V}_{max}$ indicate resting potential, overshoot, and maximum rate of phase-0 depolarization, respectively. APD_{20}, APD_{50}, and APD_{90} indicate action potential duration at 20%, 50%, and 90% repolarization, respectively. Each value is the mean ± S.E.M. from 36 experiments.

was shorter than that of the 14 – 20-day-old embryos.

E-4031 (1 μM), a blocker of I_{Kr}, significantly prolonged action potential duration at all developmental stages (Fig. 1: A, Ca). The magnitude of prolongation by E-4031 was larger in 7 – 10-day-old embryo and 11 – 13-day-old embryo than in the 14 – 20-day-old embryo and 1 – 7-day-old hatched chick. In the 11 – 13-day-old embryo, the prolongation by E-4031 was prominent and was accompanied by early after-depolarizations (EADs); phase 3 repolarization was interrupted followed by a single or a series of partial depolarization toward 0-mV level (Fig. 1Ac). Early after-depolarizations were observed in all of the preparations from the 11 – 13-day-old embryo (n = 6), but was not observed in those from other stages.

Chromanol 293B (30 μM), a blocker of the slowly activating component of the delayed rectifier K^+ current (I_{Ks}), prolonged action potential duration at all developmental stages (Fig. 1Cb); the prolongation by chromanol 293B was statistically significant, but was much smaller than that by E-4031 at all developmental stages.

Terfenadine (30 μM) produced a prolongation of the action potential duration in the 11 – 13-day-old embryo. Such prolongation was not observed at other stages (Fig. 1B, Cc).

The action potential duration of the chick ventricular myocardium increased during the embryonic period and was shortened in the hatched chick. This was in agreement with previous reports (1, 8) and also appeared to be similar to the case in the guinea pig where the action potential duration increased during the embryonic period followed by a decrease during the perinatal period (9). The developmental change in action potential duration is likely to be accompanied by changes in the balance of underlying membrane currents, as was shown to be the case in guinea pig (10). Such changes would greatly affect the responsiveness of the myocardium to pharmacological agents acting on myocardial ion channels. E-4031 markedly prolonged the action potential duration at all ages examined, while the prolongation by chromanol 293B was small (Fig. 1C). This suggests that in the chick ventricular myocardium, the rapid component (I_{Kr}), but not the slow component (I_{Ks}), of the delayed rectifier potassium channel is largely responsible for the repolarization, which is the same as in many mammalian species including the guinea pig, rabbit, and human. The prolongation by E-4031 was most prominent in the 11 – 13-day-old embryo (Fig. 1). The most likely explanation is that the prolongation of the repolarization phase of the embryonic myocardia reflects less density of repolarizing currents. In other words, the embryonic myocardia have less "repolarization reserve" (11), which makes the action potential highly sensitive to I_{Kr} blockade. Early afterdepolarizations, which are considered to be one of the causes of cardiac arrhythmia, were induced by E-4031 in all of the preparations from the 11 – 13-day-old embryo (Fig. 1Ac). In mammalian myocardia, I_{Kr} blockade is known to induce action potential prolongation, but does not always induce early after-depolarization. For example, in guinea-pig ventricular myocardium, E-4031 (1 μM) prolonged the action potential duration by about 70 ms, but did not induce early after-depolarizations (12).

Clinical treatment with certain cardiovascular and non-cardiovascular drugs has been reported to induce QT prolongation and serious ventricular arrhythmia including *torsades de pointes*. Drugs such as terfenadine and cisapride were withdrawn from clinical practice because of their arrhythmogenic risk. Since then, the assessment of the risks incurred with noncardiovascular therapeutic agents for cardiac function has received great attention (13). Terfenadine inhibits the I_{Kr} current in freshly isolated myocardial cells (14) and the hERG channel current expressed in HEK293 cells (15), but does not prolong the

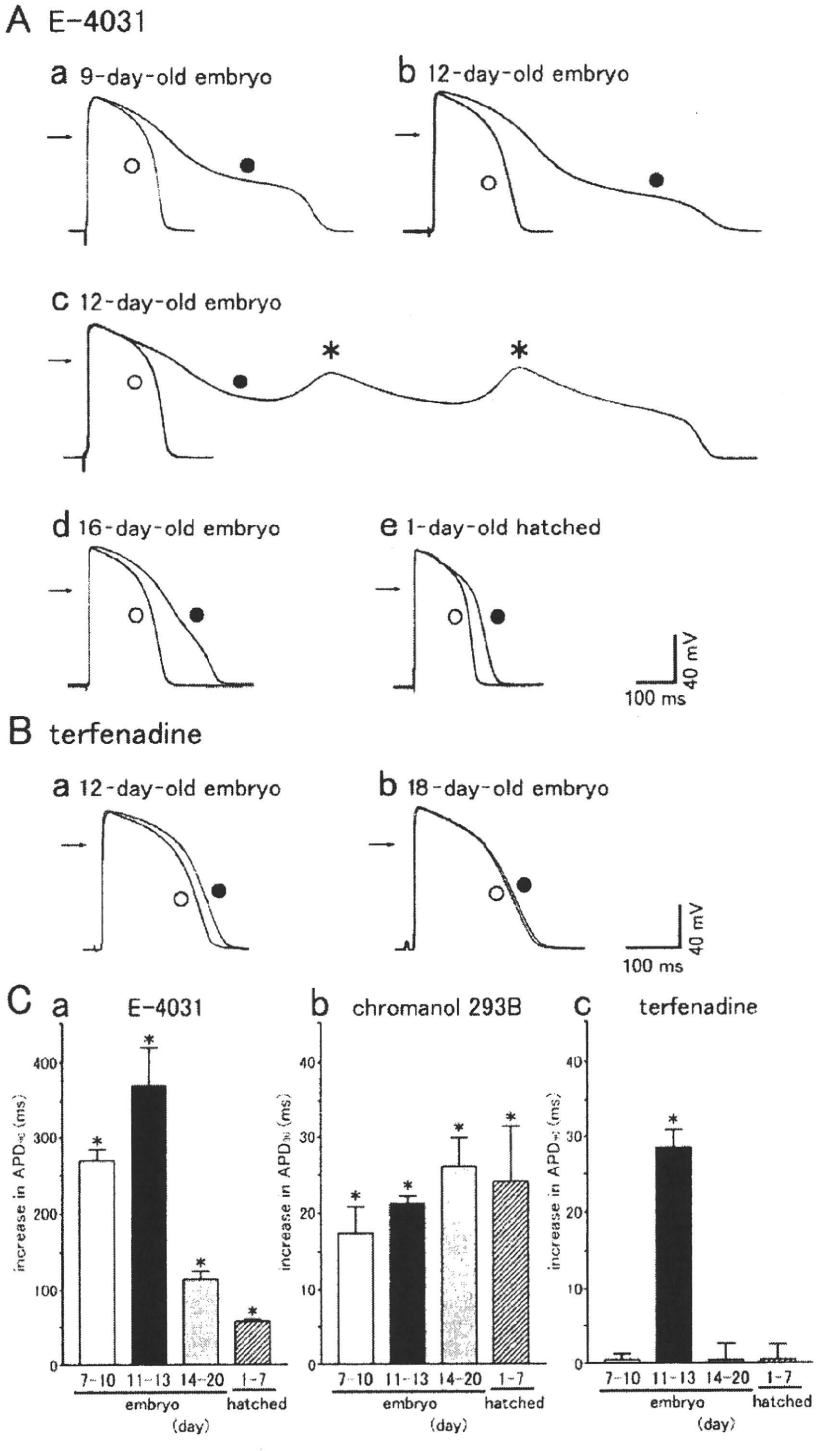

Fig. 1. Effect of K^+-channel blockers on the action potential of isolated chick ventricular myocardium. A: Typical action potential recordings before (open circles) and after (closed circles) the addition of E-4031 (1 μM) in the 9-day-old embryo (a), 12-day-old embryo (b, c), 16-day-old embryo (d), and 1-day-old hatched chick (e). Note that E-4031 induced early after-depolarizations in the 12-day-old embryo (c). B: Typical action potential recordings before (open circles) and after (closed circles) the addition of terfenadine (30 μM) in the 12-day-old embryo (a) and in the 18-day-old embryo (b). Horizontal arrows indicate zero-mV level. Voltage and time calibrations apply to all panels. C: Summarized results for the prolongation of the action potential duration at 90% repolarization (APD_{90}) by 1 μM E-4031 (a), 30 μM chromanol 293B (b), and 30 μM terfenadine (c) in the 7 – 10-day-old embryo (open columns), 11 – 13-day-old embryo (closed columns), 14 – 20-day-old embryo (gray columns), and 1 – 7-day-old hatched chick (hatched columns). Columns and vertical bars are the mean ± S.E.M. from 5 to 6 experiments. Asterisks indicate that the prolongation was statistically significant. Note the difference in the scale of the ordinate.

action potential duration in isolated ventricular tissue from mammals even at 20 μM (15,16). Such presence of "false positive" drugs complicate drug evaluation through action potential duration in tissue preparations (17).

Terfenadine did not prolong action potential duration in the 14 – 20-day-old embryo, which was the same as in isolated mammalian myocardial tissue. However, terfenadine prolonged the action potential duration in the 11 – 13-day-old embryo (Fig. 1: B, Cc). Thus, the 11 – 13-day-old chick embryonic myocardium may be a sensitive model to detect the proarrhythmic activity of drugs. Details such as the density of depolarizing and repolarizing membrane currents and the molecular structure of the delayed rectifier potassium channel in the chick ventricle await further investigation.

In conclusion, we found that the chick ventricle changes its repolarization reserve during development, which provides an interesting model for further studies on myocardial repolarization mechanisms and drug evaluation.

Acknowledgments

This study was supported in part by a Grant-in-Aid from the Ministry of Education, Culture, Sports, Science, and Technology of Japan (#21590293, #21590602, and #22790262) and the Science Research Promotion Fund from the Promotion and Mutual Aid Corporation for Private Schools of Japan. This study was performed in part as "Research on the molecular mechanisms of appearance of age-related diseases by failure of cell function control system, and their prevention and treatment" by the "Research Center for Aging and Age-related Diseases" established in the Toho University Faculty of Pharmaceutical Sciences.

References

1 Sperelakis N, Shigenobu K. Changes in membrane properties of chick embryonic hearts during development. J Gen Physiol. 1972;60:430–453.

2 Satoh H, Sada H, Tohse N, Shigenobu K. [Developmental aspects of electrophysiology in cardiac muscle]. Folia Pharmacol Jpn (Nippon Yakurigaku Zasshi). 1996;107:213–223. (text in Japanese with English abstract)

3 Nouchi H, Tanaka H, Shigenobu K. Pharmacological properties of the developing chick myocardium. Trends Comparative Biochem Physiol. 2005;11:37–45.

4 Tanaka H, Namekata I, Nouchi H, Shigenobu K, Kawanishi T, Takahara A. New aspects for the treatment of cardiac diseases based on the diversity of functional controls on cardiac muscles: diversity in the excitation-contraction mechanisms of the heart. J Pharmacol Sci. 2009;109:327–333.

5 Nouchi H, Kaeriyama S, Muramatsu A, Sato M, Hirose K, Shimizu N, et al. Muscarinic receptor subtypes mediating positive and negative inotropy in the developing chick ventricle. J Pharmacol Sci. 2007;103:75–82.

6 Tanaka H, Komikado C, Namekata I, Nakamura H, Suzuki M, Tsuneoka Y, et al. Species difference in the contribution of T-type calcium current to cardiac pacemaking as revealed by *R*(−)-efonidipine. J Pharmacol Sci. 2008;107:99–102.

7 Namekata I, Tsuneoka Y, Takahara A, Shimada H, Sugimoto T, Takeda K, et al. Involvement of the Na^+/Ca^{2+} exchanger in the automaticity of guinea-pig pulmonary vein myocardium as revealed by SEA0400. J Pharmacol Sci. 2009;110:111–116.

8 Kasuya Y, Matsuki N, Shigenobu K. Changes in sensitivity to anoxia of the cardiac action potential plateau during chick embryonic development. Dev Biol. 1977;58:124–133.

9 Agata N, Tanaka H, Shigenobu K. Developmental changes in action potential properties of the guinea-pig myocardium. Acta Physiol Scand. 1993;149:331–337.

10 Kato Y, Masumiya H, Agata N, Tanaka H, Shigenobu K. Developmental changes in action potential and membrane currents in fetal, neonatal and adult guinea-pig ventricular myocytes. J Mol Cell Cardiol. 1996;28:1515–1522.

11 Sugiyama A. Sensitive and reliable proarrhythmia *in vivo* animal models for predicting drug-induced torsades de pointes in patients with remodeled hearts. Br J Pharmacol. 2008;154:1528–1537.

12 Matsuda T, Takeda K, Ito M, Yamagishi R, Tamura M, Nakamura H, et al. Atria selective prolongation by NIP-142, an antiarrhythmic agent, of refractory period and action potential duration in guinea pig myocardium. J Pharmacol Sci. 2005;98:33–40.

13 Nakaya H, Hashimoto K. QT PRODACT: database construction for the evaluation of the risk of QT interval prolongation by drugs in Japan. J Pharmacol Sci. 2005;99:421.

14 Tanaka H, Nishimaru K, Sekine T, Shijuku T, Shigenobu K. Effects of terfenadine, betotastine and ketotifene on the action potential and membrane currents in isolated guinea-pig myocardium. Res Commun Pharmacol Toxicol. 1997;2:163–174.

15 Masumiya H, Saito M, Ito M, Matsuda T, Noguchi K, Iida-Tanaka N, et al. Lack of action potential-prolonging effect of terfenadine on rabbit myocardial tissue preparations. Biol Pharm Bull. 2004;27:131–135.

16 Tanaka H, Masumiya H, Kato Y, Shigenobu K. Inhibitory effects of terfenadine on the rising phase of action potentials in isolated guinea-pig myocardium. Gen Pharmacol. 1996;27:337–340.

17 Kii Y, Hayashi S, Tabo M, Shimosato T, Fukuda H, Itoh T, et al. QT PRODACT: evaluation of the potential of compounds to cause QT interval prolongation by action potential assays using guinea-pig papillary muscles. J Pharmacol Sci. 2005;99:449–457.

J Pharmacol Sci 115, 176 – 181 (2011)

Journal of Pharmacological Sciences

Full Paper

Electrophysiological and Pharmacological Characteristics of Triggered Activity Elicited in Guinea-Pig Pulmonary Vein Myocardium

Akira Takahara[1,*], Takahiko Sugimoto[1], Takuma Kitamura[1], Kiyoshi Takeda[1], Yayoi Tsuneoka[1], Iyuki Namekata[1], and Hikaru Tanaka[1]

[1]*Department of Pharmacology, Toho University Faculty of Pharmaceutical Sciences, Funabashi, Chiba 274-8510, Japan*

Received September 10, 2010; Accepted December 5, 2010

Abstract. The pulmonary vein is known as an important source of ectopic beats, initiating frequent paroxysms of atrial fibrillation. We analyzed electrophysiological and pharmacological characteristics of triggered activity elicited in the isolated pulmonary vein from the guinea pig. Immediately after the termination of train stimulation (pacing cycle length of 100 ms), spontaneous activities accompanied with phase-4 depolarization were detected in 43 out of 45 pulmonary vein preparations. Such triggered activities were not observed in the isolated left atrium. The incidence of triggered activity was higher at a shorter pacing cycle length (100 – 200 ms), and the coupling interval was shorter at a shorter pacing cycle length. Verapamil (1 μM), ryanodine (0.1 μM), and pilsicainide (10 μM) suppressed the occurrence of triggered activities. The resting membrane potential of the pulmonary vein myocardium was more positive than that of the left atrium. Carbachol (0.3 μM) hyperpolarized the resting membrane potential and completely inhibited the occurrence of triggered activities. These results suggest that the pulmonary veins have more arrhythmogenic features than the left atrium, possibly through lower resting membrane potential. The electrophysiological and pharmacological characteristics of triggered activity elicited in the pulmonary vein myocardium were similar to those previously reported using ventricular tissues.

Keywords: triggered activity, pulmonary vein, left atrium, membrane potential, carbachol

Introduction

Atrial fibrillation is known as the most common cardiac arrhythmia in adults, which is a major cause of stroke (1). Whereas the arrhythmia has been recognized to perpetuated by reentrant wavelets propagating in an abnormal atrial-tissue substrate, Haïssaguerre et al. found in 1998 that the origin of atrial ectopic beats was localized in the pulmonary vein myocardial sleeve of patients with drug-resistant atrial fibrillation (2). Cheung reported in 1980 that isolated pulmonary vein preparations from guinea pigs were capable of independent pace-making activity (3). Recently, electrophysiological characteristics of the pulmonary vein have been extensively analyzed in isolated rabbit or dog preparations, which show that the combination of reentrant and non-reentrant mechanisms is the underlying arrhythmogenic mechanisms of atrial fibrillation from the pulmonary veins (4 – 6).

Triggered activity is one of the well-recognized mechanisms of ectopy aggravated by an increased rate of beating (7 – 9). Tactics to raise the intracellular Ca^{2+} concentration of the ventricular tissues, such as treatment with digitalis or a low K^+ / high Ca^{2+} extracellular environment, causes an oscillatory Ca^{2+} release from the sarcoplasmic reticulum and transient depolarization after completion of ventricular repolarization (10). The delayed afterdepolarization (DAD) and resulting triggered activity have been shown to be effectively suppressed by Na^+-channel blockers, Ca^{2+}-channel blockers, and ryanodine in isolated ventricular preparations (11, 12). DAD-related triggered activity has been demonstrated in isolated pulmonary vein myocardium or its isolated cardiomyocytes (13, 14). However, fundamental electrophysiological characteristics of triggered activity have never been examined, such as the relationship between pacing rate to induce triggered activity and its incidence or coupling interval (10). In this study, to better understand the arrhythmogenic activity of the pulmonary vein

*Corresponding author. akirat@phar.toho-u.ac.jp
Published online in J-STAGE on January 18, 2011 (in advance)
doi: 10.1254/jphs.10232FP

itself, we analyzed electrophysiological and pharmacological characteristics of the triggered activity in isolated guinea-pig pulmonary vein. Triggered activity was induced by train stimulation, which is known as a useful methodology to reproducibly induce DAD-related triggered activity (10, 12, 15).

Materials and Methods

All experiments were approved by the Ethics Committee of Toho University Faculty of Pharmaceutical Sciences and performed in accordance with the Guiding Principles for the Care and Use of Laboratory Animals approved by The Japanese Pharmacological Society. The heart and adjunct lungs were isolated from male or female Hartley guinea pigs weighing 350 – 450 g. The pulmonary veins were separated from the left atrium and lung at the end of the pulmonary vein myocardium sleeve in Krebs-Henseleit solution of the following composition: 118.4 mM NaCl, 4.7 mM KCl, 2.5 mM $CaCl_2$, 1.2 mM $MgSO_4$, 1.2 mM KH_2PO_4, 24.9 mM $NaHCO_3$, and 11.1 mM glucose, gassed with 95% O_2 / 5% CO_2 (pH 7.4 at 37°C).

Histological examinations

Pulmonary veins were fixed with 10% formalin neutral buffer solution, and the segments were processed into paraffin blocks. The paraffinized tissue blocks were cut into 4-μm-thick sections and mounted on charged slides. For each paraffin block, one slide each was stained with Masson trichrome to accentuate muscle and connective tissues. A serial section was incubated with antibodies against α-smooth muscle actin (α-SMA, 1:500; Dako, Glostup, Denmark) followed by consecutive incubations with universal immuno-peroxydase polymer (Histofine®, Simple Stain Rat MAX PO MULTI; Nichirei Bioscience, Tokyo). Antibody binding was demonstrated by staining with 3,3'-diaminobenzidine tetrahydrochloride.

Microelectrode recording of action potential configuration

The luminal side of the pulmonary vein at the middle region between the ostium and the distal end of myocardial sleeve or endocardial surface of the left atrium was impaled with glass microelectrodes filled with 3 M KCl to record transmembrane potential using a microelectrode amplifier (Intra 767; World Precision Instruments, Sarasota, FL, USA). The action potential signals were monitored by an oscilloscope (CS-5135; Kenwood, Tokyo) and fed into a waveform analysis system (DSS98-type IV, from Canopus, Tokyo or PowerLab, from ADInstruments, Castle Hill, Australia). All experiments were performed at 36.5 ± 0.5°C.

Triggered activity was induced by a burst pacing of 100 train pulses at a pacing cycle length of 100, 150, or 200 ms using an electronic stimulator (SEN-2201; Nihon Kohden, Tokyo) with rectangular current pulses (3-ms duration, about 1.5 threshold) through bipolar platinum electrodes. Action potential parameters, including resting potential (RP), overshoot (OS), and action potential duration at 20% (APD_{20}), 50% (APD_{50}), and 90% (APD_{90}) repolarization, were measured under electrical stimulation at a constant frequency of 1 Hz. The action potentials of the pulmonary vein were of the fast-response type, and neither early afterdepolarizations (EADs) nor DADs were observed in the preparations electrically driven at 1 Hz.

Drugs

Verapamil hydrochloride and carbachol were purchased from Sigma-Aldrich (St. Louis, MO, USA), and ryanodine was obtained from Wako (Osaka). Pilsicainide hydrochloride was kindly provided by Daiichi-Sankyo Co., Ltd. (Tokyo). Ryanodine was initially dissolved in dimethylsulfoxide and diluted to 0.01% dimethylsulfoxide in the Krebs-Henseleit solution. Other drugs were dissolved in distilled water and small aliquots were added to the organ bath to obtain the desired final concentration. All other chemicals were commercial products of the highest available quality.

Statistical analyses

Statistical significance between means was evaluated by the one-way repeated measures analysis of variance followed by Contrasts for mean values comparison or by Dunnett's test. A P-value less than 0.05 was considered significant.

Results

Histology of the pulmonary vein

Typical photomicrographs of longitudinal sections of the left superior pulmonary vein obtained from the guinea pig are shown in Fig. 1. Vascular smooth muscle was detected on the luminal face of the pulmonary vein, whereas a myocardial sleeve was observed at mid-layer of the pulmonary vein.

Triggered activities in the pulmonary vein

Figure 2A shows a typical tracing of burst pacing-induced triggered activity in the pulmonary vein preparation. After the train stimulation at a pacing cycle length of 100 ms, spontaneous activities accompanied with phase-4 depolarization were detected in 43 out of 45 pulmonary vein preparations. On the other hand, phase-4 depolarization was not detected in the left atrium prepa-